



EXPLICIT DYNAMIC CRASH ANALYSIS OF A CAR BODY BY DIFFERENT LIGHTWEIGHT MATERIALS USING ANSYS

TEAM MEMBERS:

D. SIRI VENKATA NAGA GOPI(20761A0358)

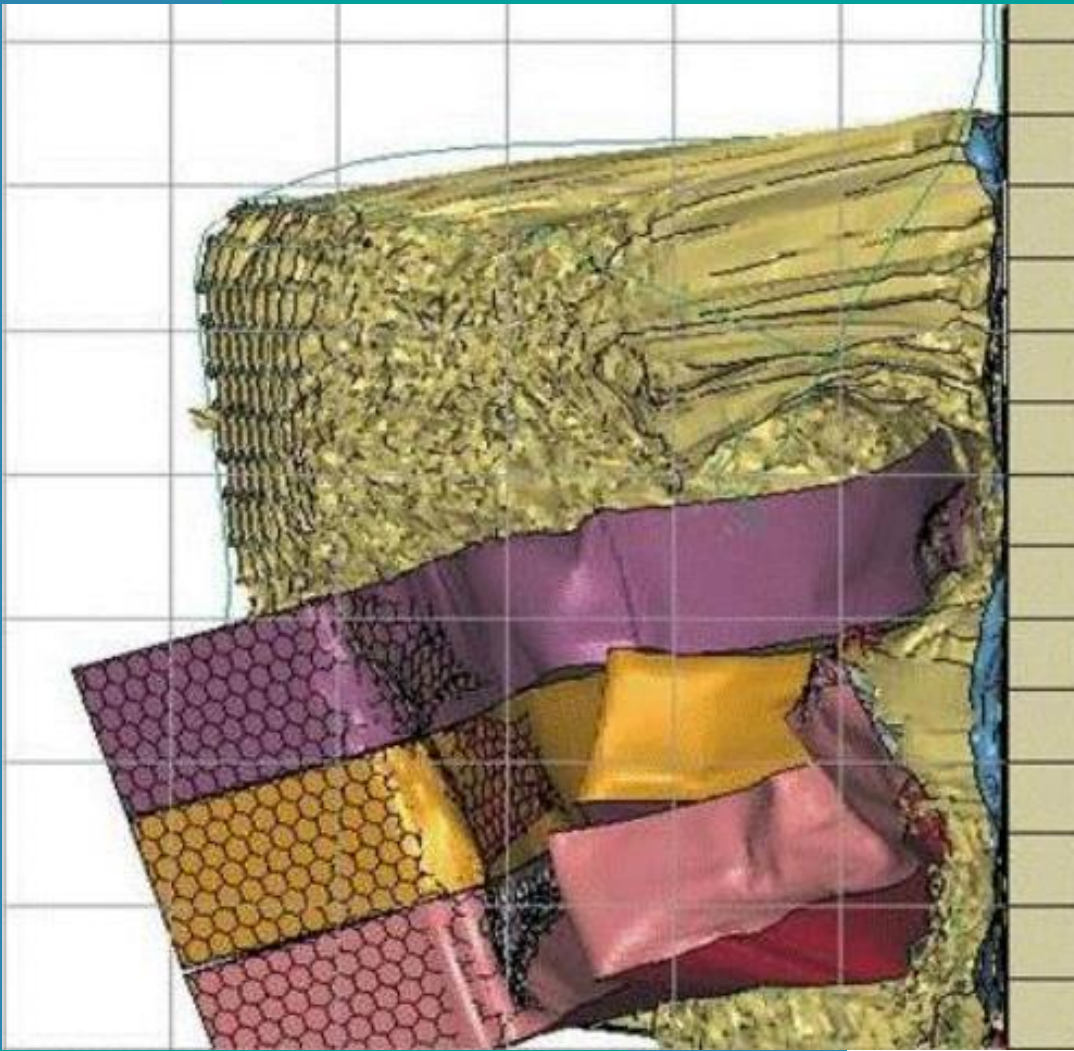
S. JAGADHISH REDDY(20761A0385)

M. KIRAN KUMAR(20761A0372)

UNDER THE GUIDANCE OF:

DR. CH. SIVA SANKARA BABU,

Associate Professor



CONTENTS:

- Abstract
- Introduction
- Literature Review
- Methodology
- Design of Car body
- Pre-processing
- Solving
- Post-processing (or) Results
- Conclusions
- References

ABSTRACT

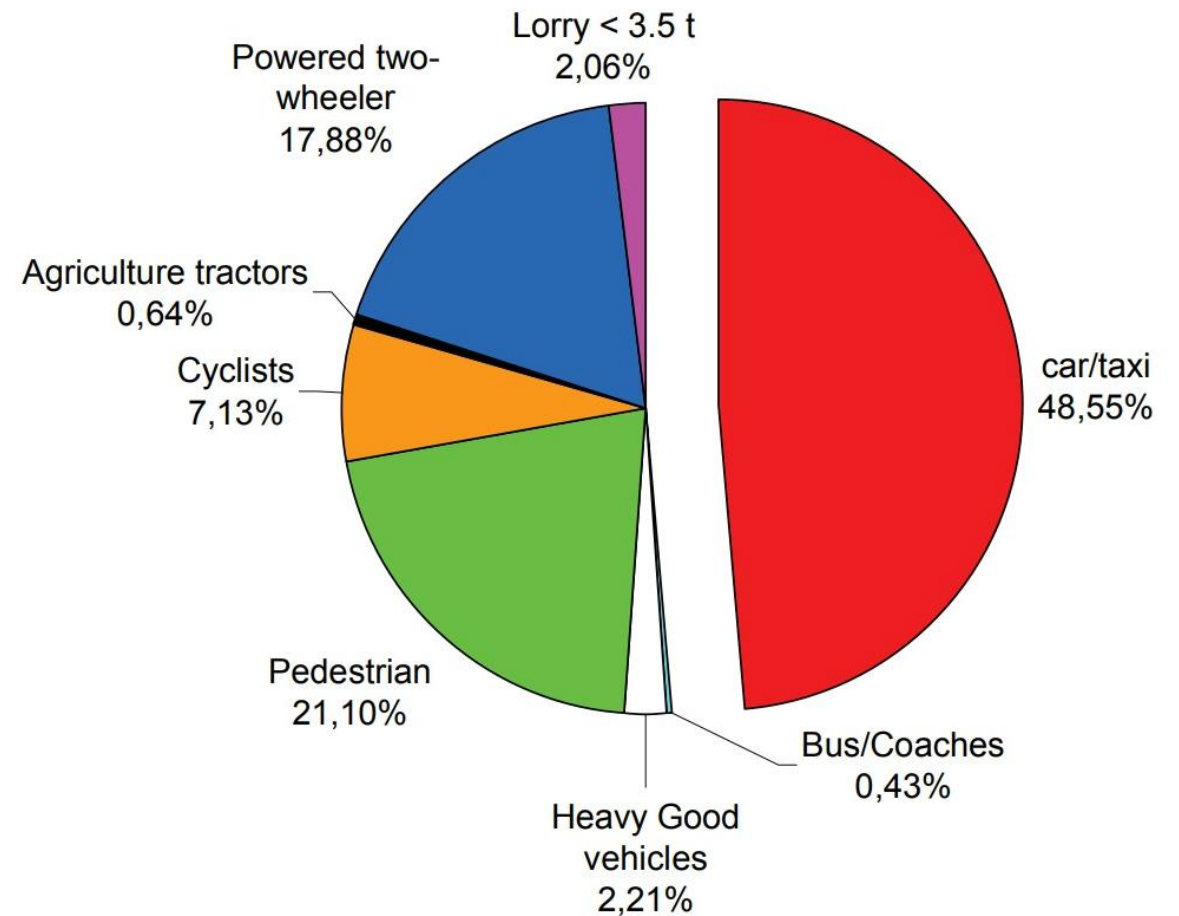
The need for materials with high strength and low weight for structural applications is growing daily. Reduced weight, lower emissions, and safer cars are top priorities, particularly for the transportation sectors like aerospace and automotive. Carbon fibers, Ti-6Al-4V, Al 7075-T6, and other light metals and alloys can all be used to reduce the weight of an automobile body. These materials tend to replace high-weight materials for some body parts, such as side doors and bonnets, in automobile manufacturing because of their high elastic modulus, high strength, and high resistance to corrosion while maintaining the body's weight relatively low. In this research the best lightweight material for the car body is sorted out of the above-mentioned materials by conducting crash test analysis of the car body through Explicit Dynamics module of the ANSYS software tool with the inbuilt solver AUTODYN. A conceptual design a coupe car body is designed through generative shape design in CATIA V5R21 software tool and that model is used in this study for conducting various crashes with a rigid barrier of material concrete, focused on three distinct crash scenarios - frontal impact, pole impact, and roll over impact at velocities 80 m/s, 50 m/s, and 36 m/s respectively. Also, this project focuses on a real-time simulation of car-to-car crash test analyses to observe the crashworthiness of a car body with another with velocities 20 m/s and 100 m/s respectively. The research evaluates the performance of different lightweight materials within these scenarios. The primary objective is to ascertain the most suitable lightweight materials for enhancing car safety and structural integrity. By conducting simulations at varying velocities and utilizing diverse lightweight materials, this study aims to determine the optimal lightweight material choices for mitigating impact forces and safeguarding occupants during collisions. The outcomes of this research provide valuable insights into lightweight material selection and crash performance assessment in automotive engineering, aiding in the design of safer vehicles.


INTRODCTION

Use of Lightweight Materials on
Car Body.



- Car accidents caused by excessive traffic that occur worldwide endanger human life safety.
- The installation of safety features has continued to be one of the top priorities for auto manufacturing companies as a preventive measure in light of such concerns.
- But regrettably, the graph showing the number of fatalities from crashes and accidents shows an upward trend.





The reduction of car body weight and structure design are pivotal in car crash safety. Here's how:

- Improved Energy Absorption
- Enhanced Structural Integrity
- Optimized Occupant Protection
- Improved Handling and Performance

Overall, while reducing car body weight is essential for fuel efficiency and performance, it also plays a vital role in enhancing crash safety when combined with advanced engineering and safety technologies.

MATERIALS USED FOR REDUCING WEIGHT OF CAR BODY

1. Al-7075T6:

- Tensile Strength: Approximately 570 MPa
- Density: Approximately 2.81 g/cm³
- Composition: Aluminium alloy with zinc as the primary alloying element, along with small amounts of magnesium, copper, and chromium.
- Strength-to-Weight Ratio≈**203 MPa·cm³ /g**

2. Ti-6Al-4V:

- Tensile Strength: Approximately 1000 MPa.
- Density: Approximately 4.43 g/cm³.
- Composition: Titanium alloy composed of 90% titanium, 6% aluminium, and 4% vanadium.
- Strength-to-Weight Ratio≈**225 MPa·cm³ /g**

3. CFRP T700 FIBER:

- Tensile Strength: Approximately 2860 MPa.
- Density: Approximately 1.80 g/cm³.
- Composition: Carbon, Na + K, Epoxy, phenolic, polyester, vinyl ester, Vinyl ester, compatible with epoxy
- Strength-to-Weight Ratio≈**1588 MPa·cm³ /g**

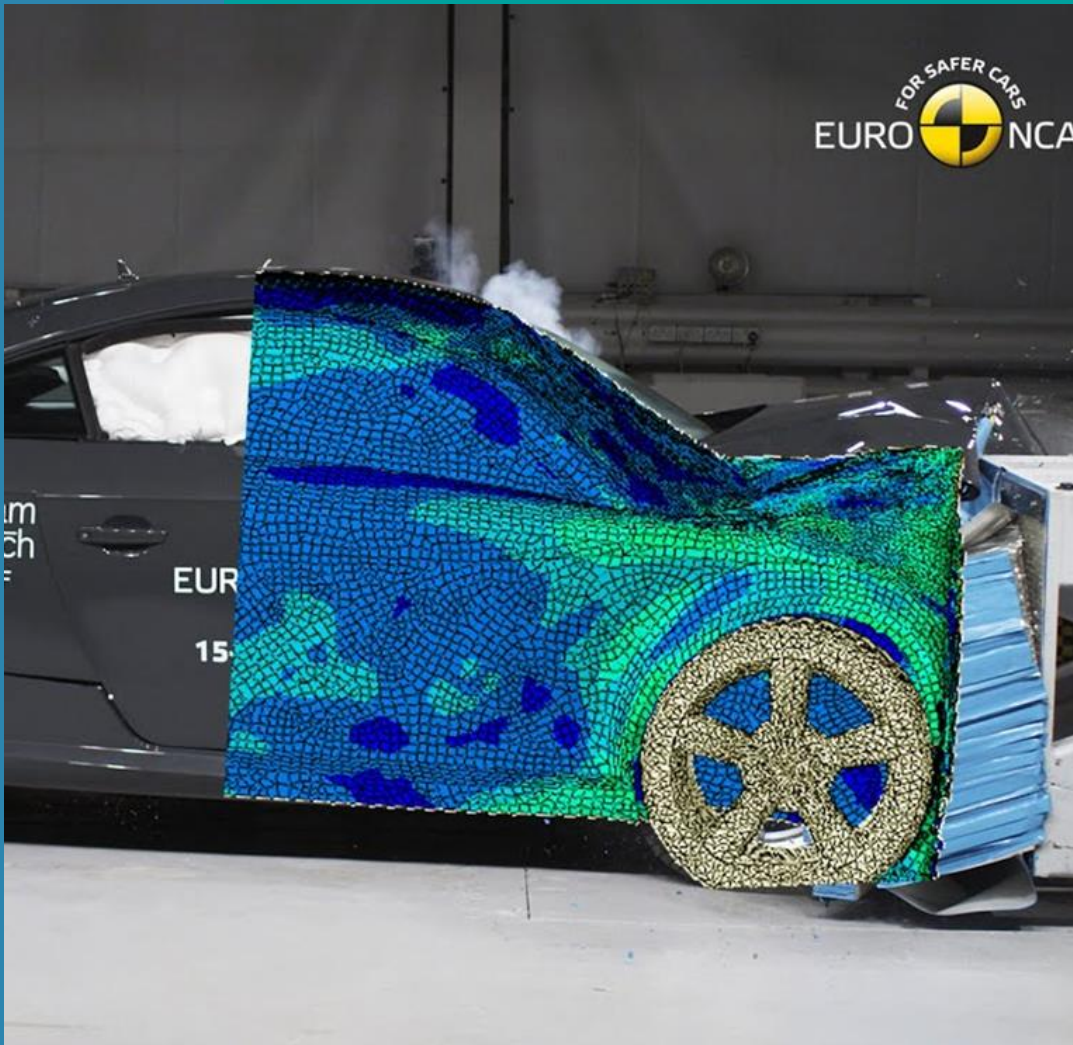
CRASH TEST ANALYSIS

- Evaluation of how a vehicle (or) its components perform (or) withstand during a collision (or) impact to a rigid (or) deformable barrier.
- Primary goal is that the safety of vehicles and passengers in it.

TYPES OF CRASH TESTS:

- 1.) Frontal impact testing
- 2.) Side impact testing
- 3.) Rollover impact testing
- 4.) Rear impact testing

- There are some special cases like Pole impact, overlap impact, car-to-car impact, computer model impact, etc., which can be crashed in the above-mentioned plane of crashes. These special cases are the subsets of the above-mentioned impact testings.



BARRIERS IN CRASH TEST

DEFORMABLE BARRIER



- Deformable barrier is a mimic object of a body (or) structure to be collided, where crash of the barrier is bothered a lot, which can absorb energy upon impact.
- E.g.: Two cars colliding each other.



RIGID BARRIER

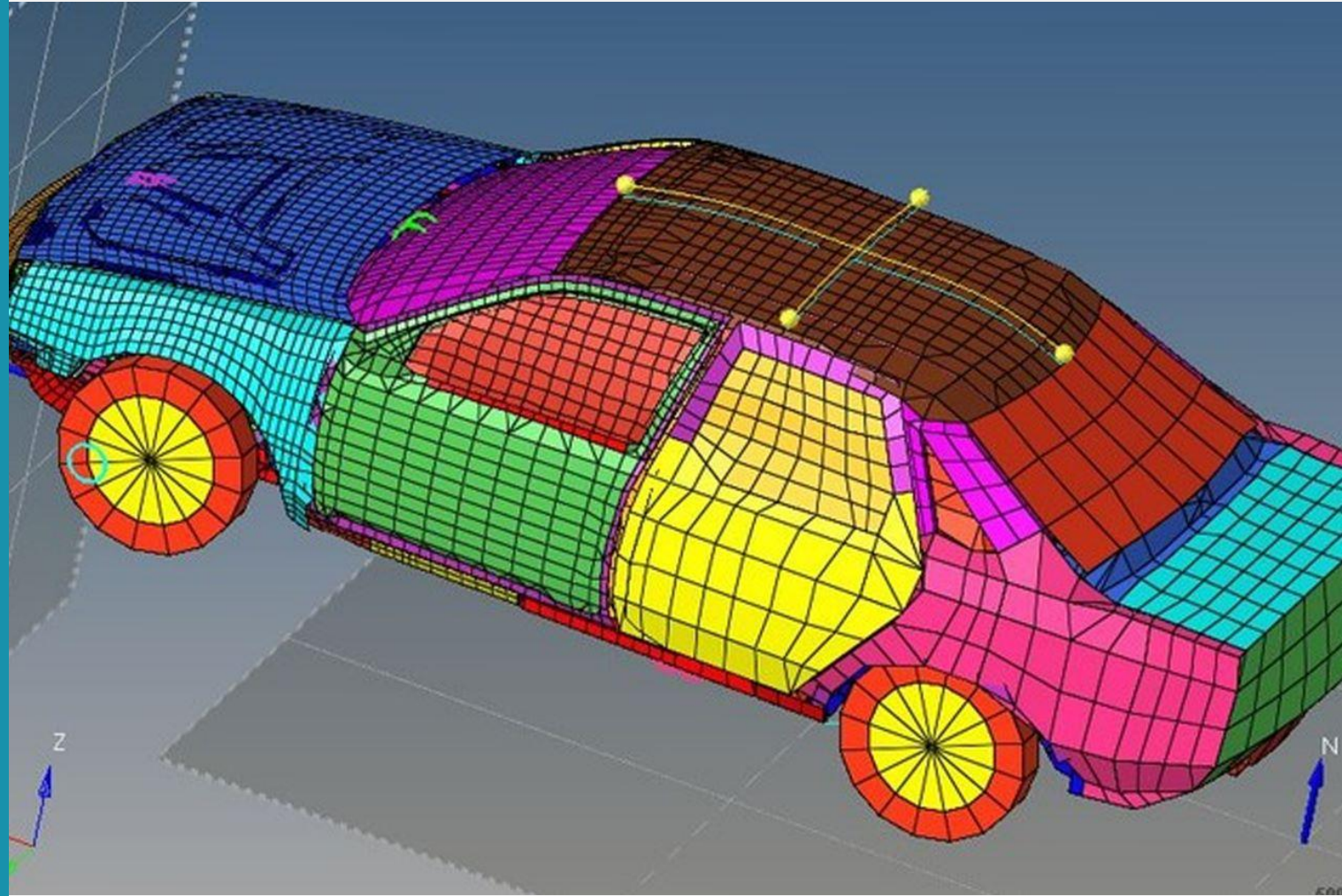
- Rigid barrier is a solid, immovable object made of materials like concrete (or) steel (or) an object where crash of barrier is least bothered about.
- E.g.: Concrete wall etc.

EXPLICIT DYNAMICS IN ANSYS

- The crashworthiness of a car model can be obtained by analyzing the crash dynamically with respect to time. Explicit Dynamic analysis is such type of analysis that is used to analyze the body's transient dynamic events, such as impacts, crashes, explosions, and other high-speed interactions, with respect to time. ANSYS proves to be an efficient software tool that handles the explicit dynamics of a body with a promising in-built solver, AUTODYN. AUTODYN provides the ability to represent a wide range of boundary conditions, contact interactions, and complicated material behaviors—all of which are essential for precise crash analysis of automobile bodies.
- Unlike implicit dynamic analysis, which iteratively solves equations of motion over time, explicit dynamic analysis discretizes time into small increments, allowing for accurate representation of high-speed and highly nonlinear events. In this approach, the equations of motion are integrated explicitly at each time step, making it particularly well-suited for simulating phenomena characterized by rapid changes and material failure.

METHODOLOGY

Numerical Method - FEM



METHODS TO SOLVE AN ENGINEERING PROBLEM

- **EXPERIMENTAL METHOD**

Solving the problem by conducting some practical sessions.

DRAWBACKS:

Initial cost, specimen, space occupied by an experimental setup, an experimental setup is used only for its respective practical session.

- **ANALYTICAL METHOD**

Solving using mathematical equations and conducting some statistical surveys.

DRAWBACKS:

This method is only suitable for small problems. It takes a lot of time to solve a complex body and requires a huge knowledge on solving problems using formula itself.

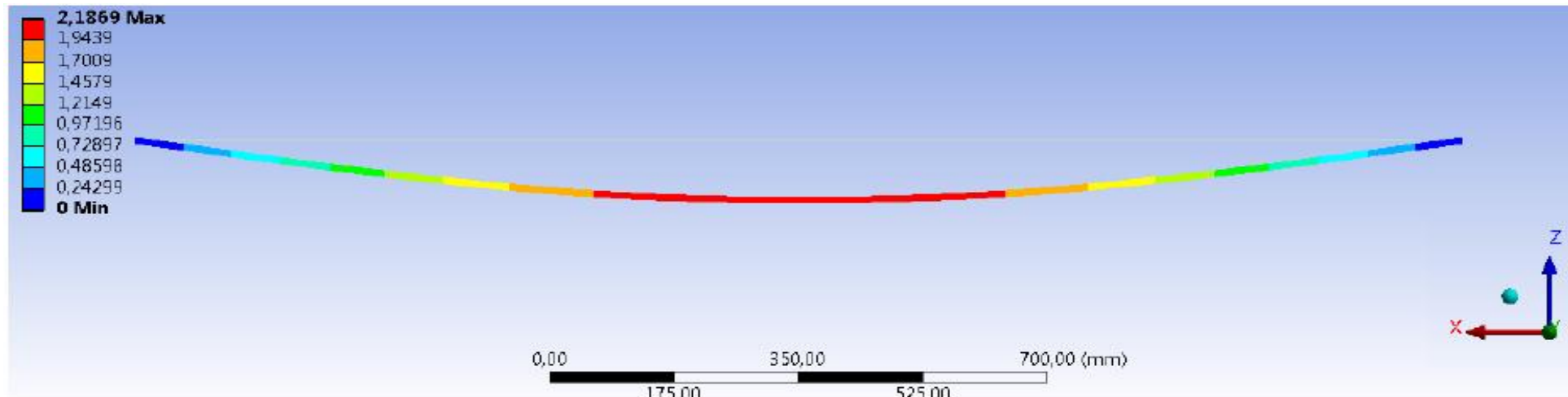
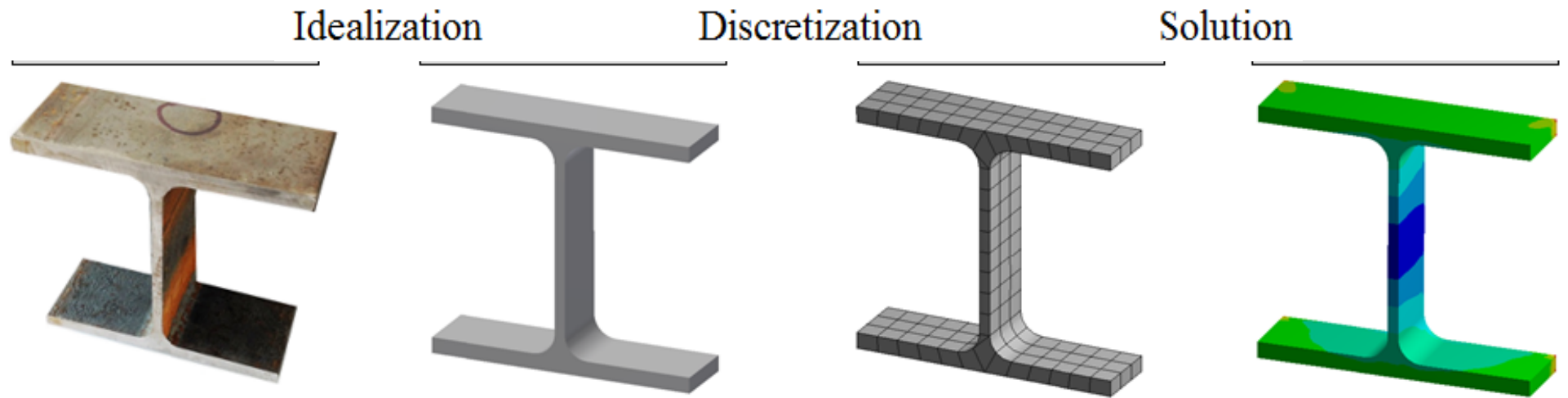
- **NUMERICAL METHOD**

Solving using the software tools by conducting different analysis like FEA, CFD etc.

DRAWBACKS:

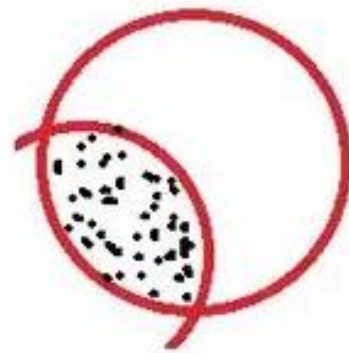
Numerical methods may not give exact analytical solutions. It gives approximate solutions.

Finite element method

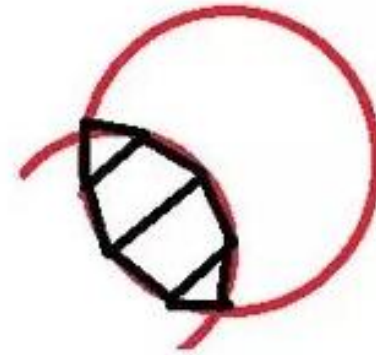


MESH

DOF



No. of nodes = infinite
Deg. of freedom = 6 for each node
No. of equations = infinite

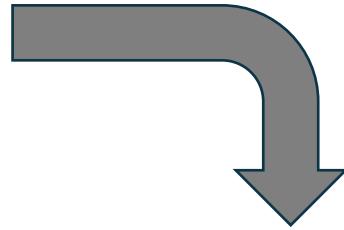


No. of nodes = 8
Deg. of freedom = 6 for each node
No. of equations = 48

PHASES OF FEM

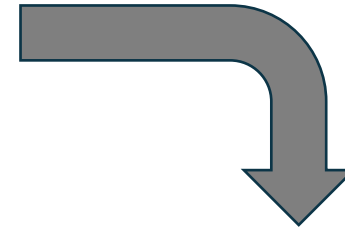
PRE-PROCESSING

- GEOMETRY
- MESH
- MATERIALS
- LOADS
- BOUNDARY CONDITIONS



SOLVING

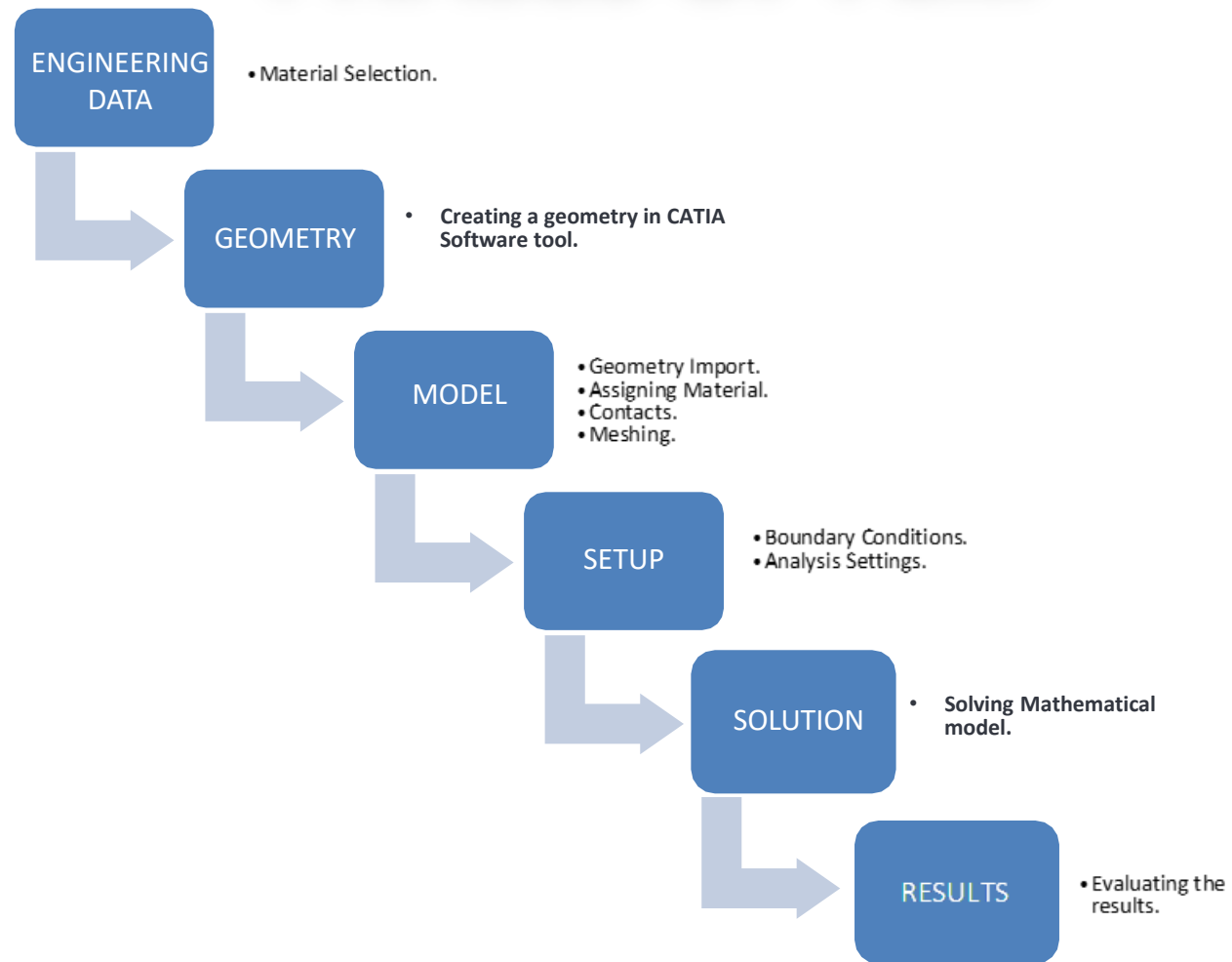
- SOLUTION



POST-PROCESSING

- EQUIVALENT STRESSES & STRAINS
- DEFORMATIONS
- FACTOR OF SAFETY

PHASES OF FEM



MATHEMATICAL MODEL

The model of the car is an impact-impulse problem. A portion of the initial kinetic energy is transformed into strain energy (elastic and plastic energy) during the crash energy transfer. An analysis of material deformation has been conducted using the Johnson-Cook plasticity model.

1. Impulse-momentum and Kinetic energy:

The following lists the mathematical relationships for impulse-momentum, which include forces, mass, and velocity between two interacting bodies:

$$\int_{t_i}^{t_f} F. dt = m. (V_i - V_f) \quad (1)$$

"F" stands for applied force, "dt" for differential time, "m" for the mass of the object being considered, and "Vi & Vf" for initial and final velocities in Eq. (1).

The following is an explanation of the law of conservation of energy:

$$\frac{1}{2}m. (V_i^2 - V_f^2) = E_{damping} + E_{elastic} + E_{plastic} = E_{Kinetic} \quad (2)$$

Equation (2) depicts the change of the car's kinetic energy into different types of energies as a result of the collision.

Given the assumption that colliding bodies are rigid, variables like as heat dissipation, acoustics, etc., can be disregarded. As a result, we obtain

$$E_{Kinetic} = \frac{1}{2}m. (V_i^2 - V_f^2) \quad (3)$$

MATHEMATICAL MODEL

2. Johnson-Cook Strength:

A plasticity/deformation model known as the Johnson-Cook plasticity model, with parameters like "strain hardening, strain rate hardening, and thermal softening," is provided by Johnson and Cook as an example of the parameters like yield stress for the materials subjected to high strain, strain rates, and temperatures. Flow stress is determined by multiplying the effective plastic strain (ϵ_p), the rate of effective plastic strain ($\dot{\epsilon}_p^*$), and the temperature (T). One way to express yield stress is as:

$$\sigma_y = [A + B \cdot \epsilon_p^n] + \left[1 + C \cdot \ln\left(\frac{\dot{\epsilon}_p^*}{\dot{\epsilon}_0^*}\right)\right] + \left[1 - \frac{T - T_r}{T_m - T_r}\right]^m \quad (4)$$

"A" represents the initial yield stress, "B" the strain hardening co-efficient, and "n" the strain hardening exponent in equation (4). The rate of plastic strain is denoted by ($\dot{\epsilon}_p^*$), the reference strain rate is denoted by ($\dot{\epsilon}_0^*$), and the reference strain rate co-efficient is denoted by "C." "m" stands for the thermal softening parameter. The following lists the Johnson-Cook model parameters for the materials.



Literature Review

LITERATURE REVIEW

S.NO.	AUTHOR	YEAR	COMPLETED WORK
1.	SUN Hongtu, SHEN Guozhe, HU Ping	2009	Developed a method for lightweight optimization of car body design based on crash simulations. Optimized car body part thicknesses to minimize weight while maintaining stiffness and crash safety. Validated safety performance through crash simulations and adjusted part thicknesses to meet safety requirements.
2.	Tejasagar Ambati, K.V.N.S. Srikanth, P. Veeraraju	2012	Conducted frontal crash test simulations to validate results and explore material modifications for reducing crash forces. Analyzed crash characteristics of a Chevrolet C1500 pick-up truck using LS-DYNA software and compared results with NCAC test data, demonstrating the reliability of computer simulations in assessing vehicle crash performance.
3.	T. Ananda Babu, D. Vijay Praveen, Dr. M. Venkateswarao	2012	Investigated car crash responses, focusing on chassis frame behavior during frontal impacts using ANSYS simulations. Analyzed frame deformation and stress distribution to ensure adequate passenger protection, highlighting the importance of using technology to enhance vehicle safety.

S.NO.	AUTHOR	YEAR	COMPLETED WORK
4.	Heiko Johannsen et al.	2012	Explored vehicle safety during frontal collisions and proposed a method for evaluating crash compatibility between vehicles. Combined crash tests and numerical simulations to develop test procedures for assessing frontal impact safety and compatibility. Aimed to enhance vehicle safety standards and promote compatibility between vehicles involved in frontal collisions.
5.	Yu ZHU, Li LI, JiKuang YANG	2012	Focused on improving frontal structure energy absorption during low-speed crashes by optimizing the crash-box. Conducted simulations based on RCAR regulations to design a crash-box that effectively met safety requirements, demonstrating the effectiveness of their approach in enhancing vehicle safety.
6.	Guibing LI, Jikuang YANG	2012	Explored the impact of vehicle front structure on compatibility in car-to-SUV frontal crashes through simulations. Analyzed compatibility across different overlap ratios to enhance both vehicles' compatibility performance, highlighting the importance of structural design in mitigating crash impacts and improving overall vehicle safety.

S.NO.	AUTHOR	YEAR	COMPLETED WORK
7.	Zeng Biqiang, Xue Shugang, Fang rui	2013	Investigated car crash response to moving distorted barriers (MDB) and proposed structural changes to enhance vehicle safety and compliance with international standards. Analyzed disciplinary differences in crash dynamics and prompted new decisions regarding car body structural components to improve safety.
8.	Xuemei Wang, Jun Shi	2013	Validated the Johnson-Cook constitutive relation and failure criterion for Ti-6Al-4V under high strain rates through experimental and numerical methods. Demonstrated good agreement between experimental measurements and numerical predictions, confirming the validity of the Johnson-Cook model for capturing material behavior under impact loading.
9.	Chunke Liu, Xinping Song, Jiao Wang	2014	Simulated car front collisions using LS-DYNA and Hyper Work software to evaluate anti-impact capability and structural design's role in enhancing vehicle safety. Analyzed deformation and acceleration curves during crash simulations to assess crashworthiness and inform design decisions aimed at improving vehicle safety.

S.NO.	AUTHOR	YEAR	COMPLETED WORK
10	Akshay P. Lokhande et al.	2016	Analyzed vehicle crash dynamics to evaluate chassis crashworthiness and optimize chassis design using FEA. Demonstrated the practical application of computational methods in enhancing vehicle safety while meeting performance and efficiency goals.
11	Erika Fečovaa et al.	2016	Calculated deformation work and biomechanical limits in car frontal crashes to identify ideal materials for car construction. Proposed material selection criteria to minimize injuries while safeguarding the car's structure, contributing to enhanced car safety.
12	C. Sai Kiran, J. Sruthi, S. Chandrahas Balaji	2017	Conducted crash analysis of a passenger car using ANSYS Workbench software to evaluate car body deformation and crashworthiness. Demonstrated the importance of advanced simulation techniques in optimizing vehicle safety and informing design improvements.

S.NO.	AUTHOR	YEAR	COMPLETED WORK
13.	Andrew Hickey, Shaoping Xiao	2017	Used finite element modeling to simulate car crashes and accurately predict crash outcomes. Analyzed various incoming speeds and their impact on car behavior during collisions, offering insights into vehicle design and safety standards.
14.	Taisuke Watanabea et al.	2019	Investigated the correlation between frontal car-to-car (C2C) test outcomes and vehicle crash compatibility evaluations. Developed refined test methods to ensure consistent evaluations of occupant safety in C2C impact scenarios, contributing to improved vehicle safety standards.
15.	Mohammed Abdul Basith et al.	2020	Enhanced passenger car bumper assembly design through crash analysis to improve impact test performance. Identified suitable materials and designs for effective impact energy absorption and passenger safety, contributing to improved car safety.

S.NO.	AUTHOR	YEAR	COMPLETED WORK
16.	Babalu Kumar et al.	2021	Evaluated composite car body crash performance using Ansys Workbench software and explored the potential benefits of using composite materials in car body construction. Demonstrated the feasibility of enhancing car safety and performance while optimizing fuel efficiency through material selection and design improvements.
17.	Soniya Patil, Rutuja Wani, Sudhakar Umale	2022	Analyzed explicit dynamics crash scenarios of cars made from different materials to determine crashworthiness. Investigated stress and deformation development in various crash scenarios to inform material selection and design improvements for enhanced vehicle safety.
18.	Diana Goncharovaa et al.	2022	Developed a method for evaluating fatigue damage stages of sheet structural materials to enhance car body design maintainability and safety. Conducted fatigue tests on different steel grades to identify materials suitable for car body construction, contributing to improved car safety and longevity.

S.NO.	AUTHOR	YEAR	COMPLETED WORK
19	Imtiaz Shah et al.	2022	Investigated ballistic impact behavior of auxetic sandwich composite human body armor using FEA. Analyzed armor response to various projectile velocities to evaluate protection capabilities and compared performance with conventional monolithic body armor, highlighting the potential of auxetic armor for enhanced ballistic protection.
20	Bin Wu et al.	2022	Analyzed the impact of flocking bird strikes on engine fan blades using numerical simulation. Investigated blade deformation and dynamic responses to different flocking bird sizes and impact locations, providing insights into potential damage and risk to rotor systems during bird strikes.
21	Usama Idrees et al.	2023	Optimized car frame materials to enhance safety through crash simulations. Analyzed frame performance against frontal impacts and evaluated passenger zone deformation at various velocities, aiming to mitigate casualties in car accidents while ensuring fuel efficiency.

PROBLEMS IDENTIFIED:

As observed from the previous works done on the car crash analysis using Numerical method, some problems are identified, such as:

- ❑ The car crash analysis in simulation software of the Coupe car body type, which is a sport utilized car body, had not done in the previous studies, rather than they covered SUVs, sedans etc.
- ❑ The car crash analysis was done only in one plane of crash, rather than conducting the crash test in different plane of crashes at higher speeds.

OBJECTIVES OF PRESENT WORK:

To study:

- Crash worthiness of a Coupe car body.
- For sorting out the best lightweight material for Coupe type of car body.
- Car Crash analysis in ANSYS using explicit dynamics, in Frontal, Side(pole), and Rollover plane of crashes with a rigid barrier.
- Car-to-car crash test analysis of the coupe car body, in frontal and side planes.

The below-mentioned tests were done on the car body, for three materials. Total no. of analyses would be 15.

- **TEST1** : Frontal Barrier Impact Test.
- **TEST2** : Side (Pole) Barrier Impact Test.
- **TEST3** : Rollover Barrier Impact Test.
- **TEST4** : Car-to-Car Frontal Impact Test.
- **TEST5** : Car-to-Car Side Impact Test.

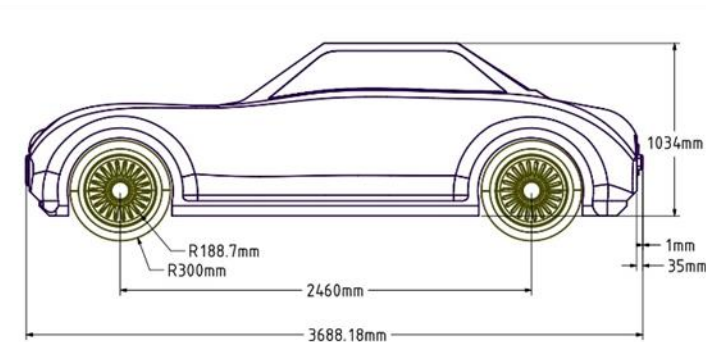
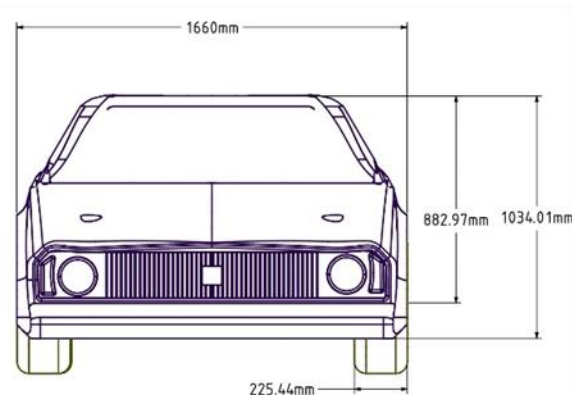
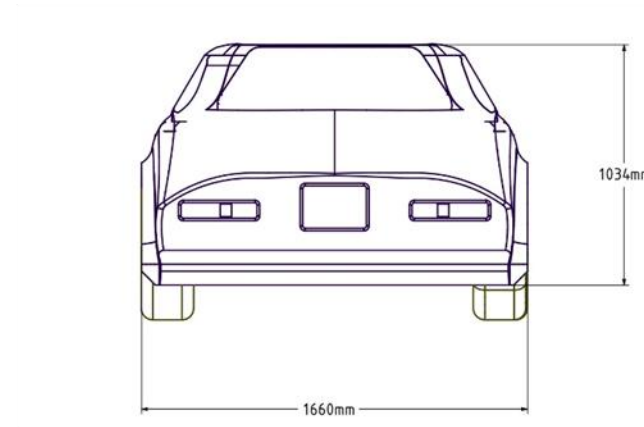
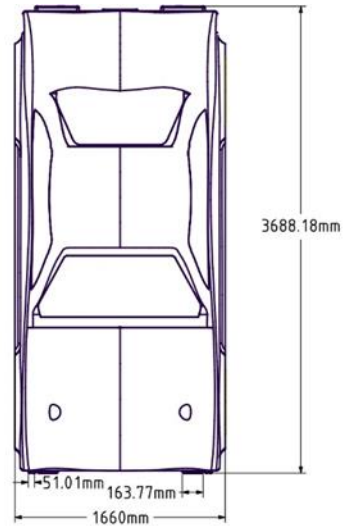
DESIGN OF CAR BODY

Conceptual Design using CATIA.
Building Barriers using Space Claim.

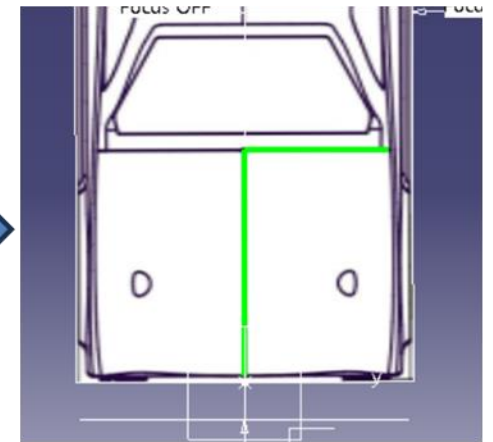
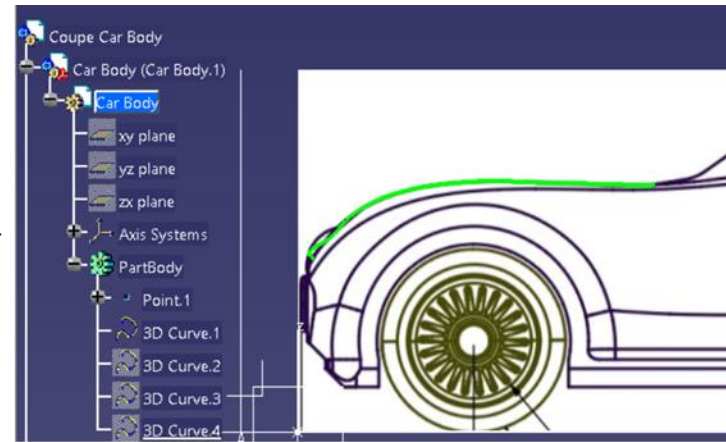
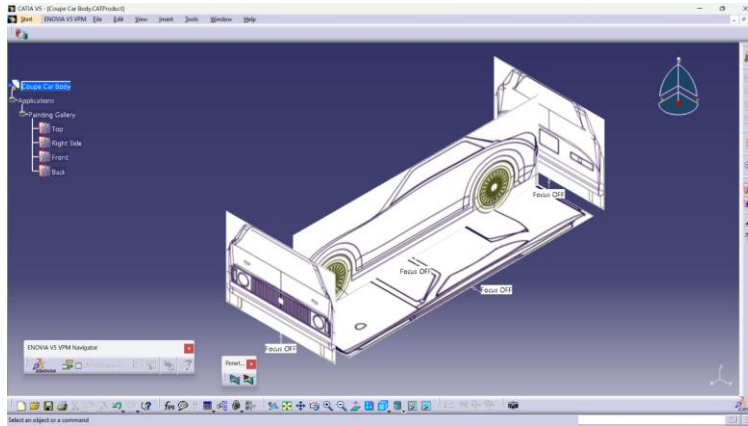


DESIGN OF CAR BODY

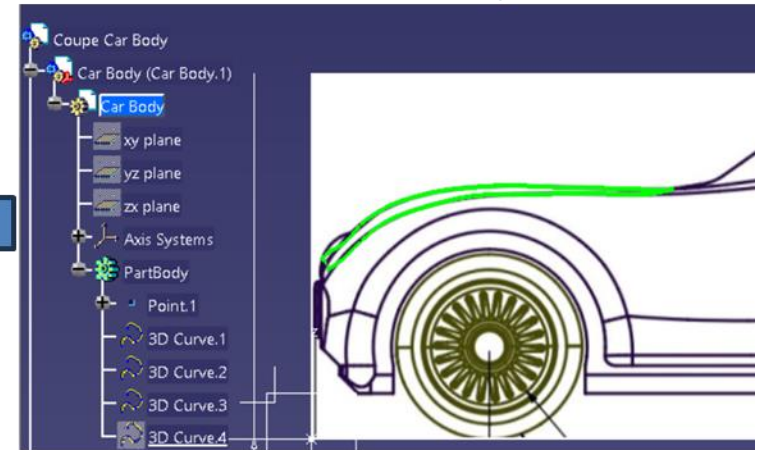
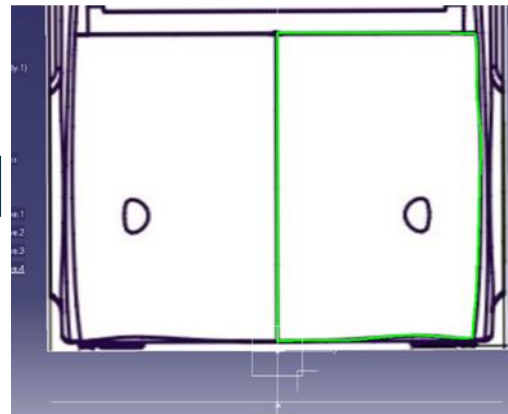
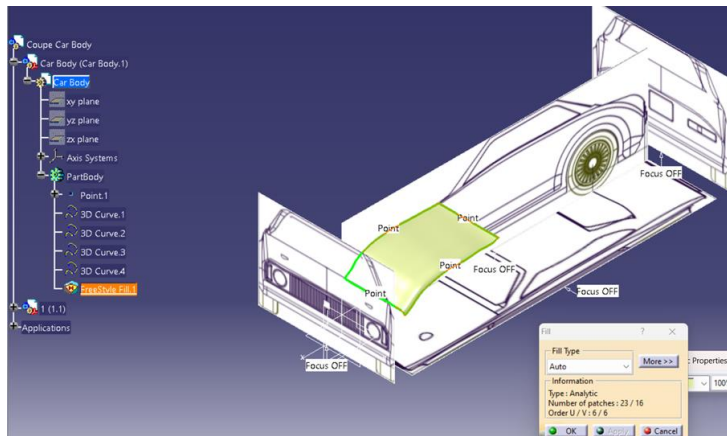
- The conceptual design of the car body was done using the CATIA V5R21 software with the help of given blueprints.



DESIGN OF CAR BODY: CATIA



- Graphical abstract of creating a 3D curve from 3D lines, using the geometry available on the background in CATIA V5R21.



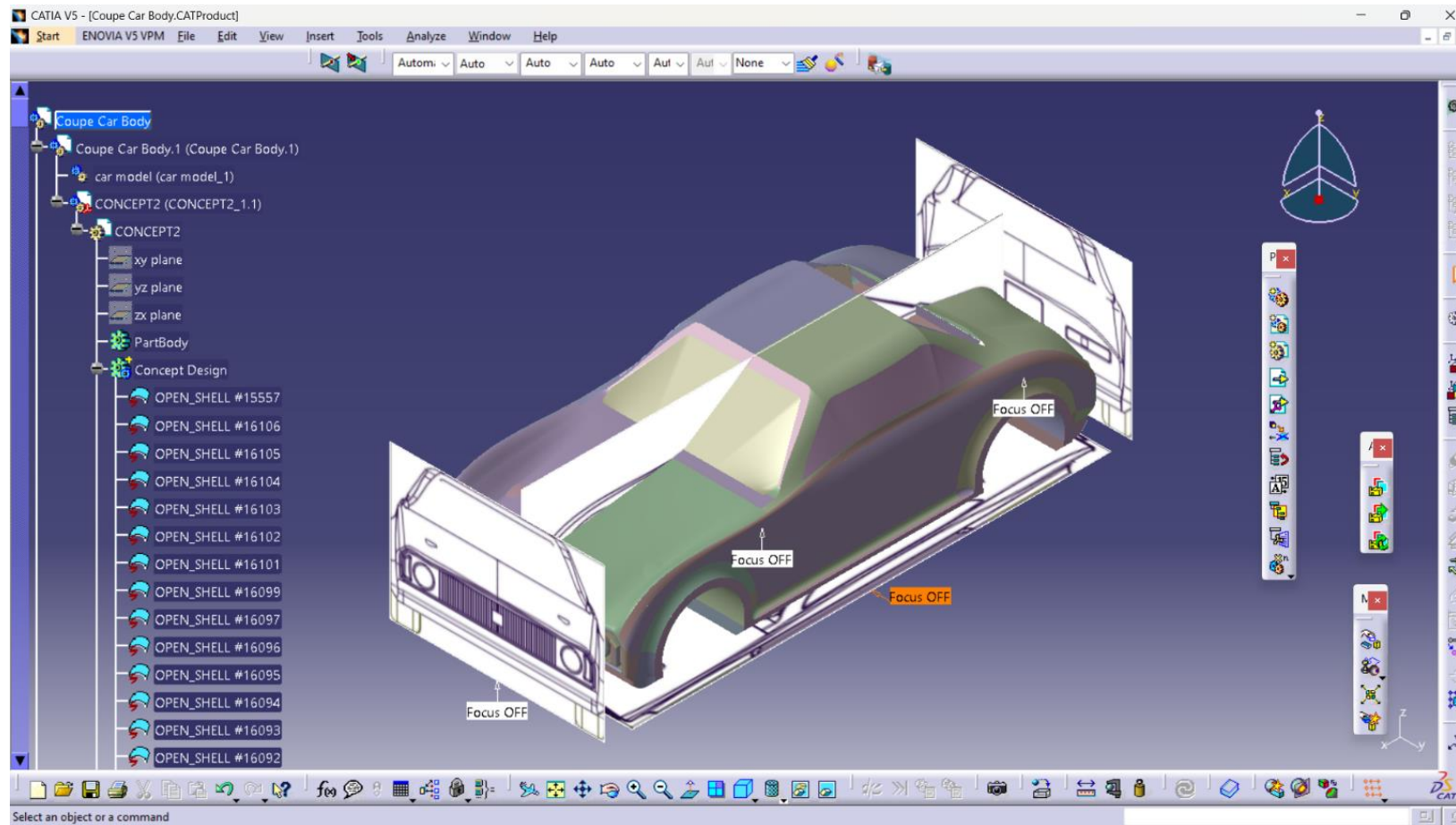
DESIGN OF CAR BODY: CATIA

Steps to create 3D curves and surfaces:

- Enable “Make Privileged Plane Most Visible” by clicking left button of mouse, on the triad.
- Replicate a 3D curve from the positioned images in space, using the command, “3D Curve”, from the toolbar, “Curve Creation.”
- Assign a typical colour for the 3D curve and a curve thickness of 4.01mm, using the “Graphic Properties”, to find the drawn images well.
- Make sure the created group of curves make a closed profile.
- Create a surface from a group of surfaces using the command, “FreeStyle Fill” from the toolbar, “Surface Creation.”

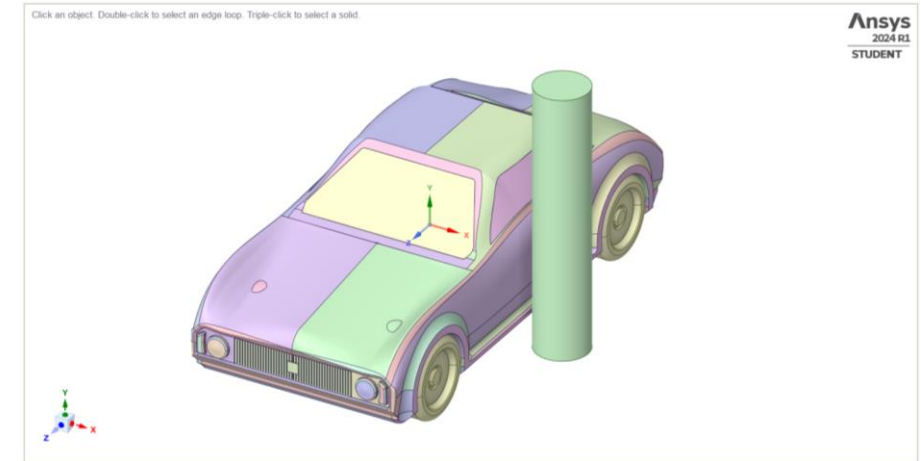
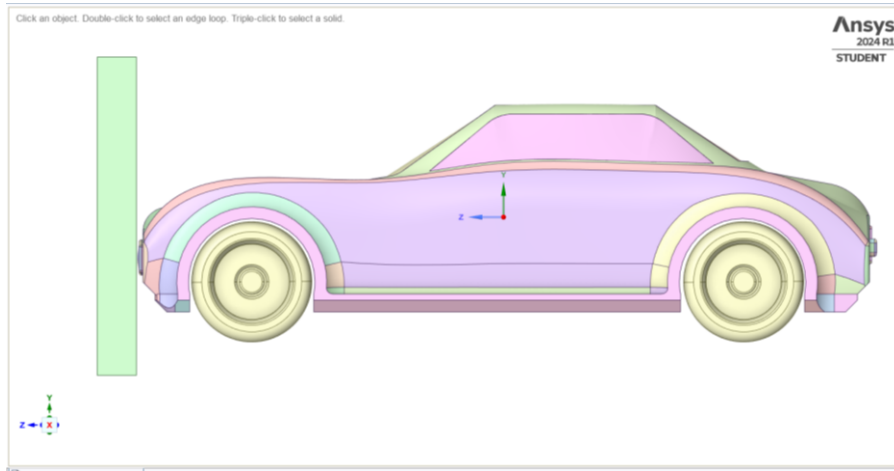
DESIGN OF CAR BODY: CATIA

- Final product of the conceptual design of the coupe car body,



DESIGN OF CAR BODY: SPACE CLAIM

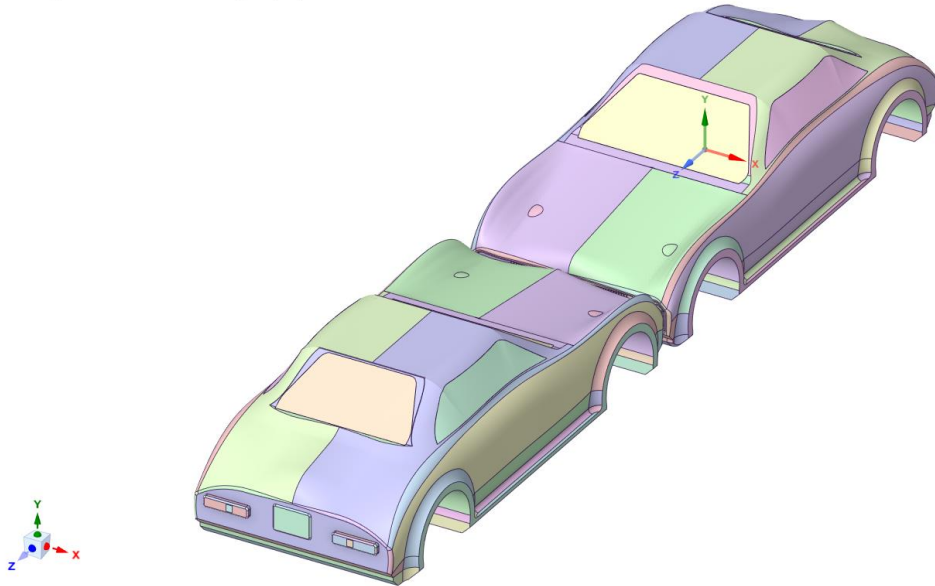
- Coupe Body design with rigid barriers.



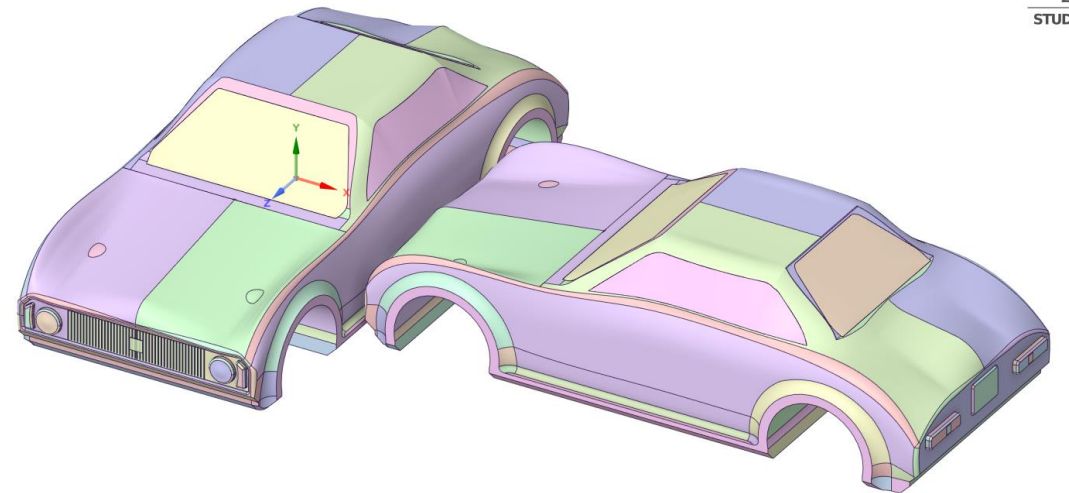
DESIGN OF CAR BODY: SPACE CLAIM

- Coupe Body design with Car-to-car.

Click an object. Double-click to select an edge loop. Triple-click to select a solid.

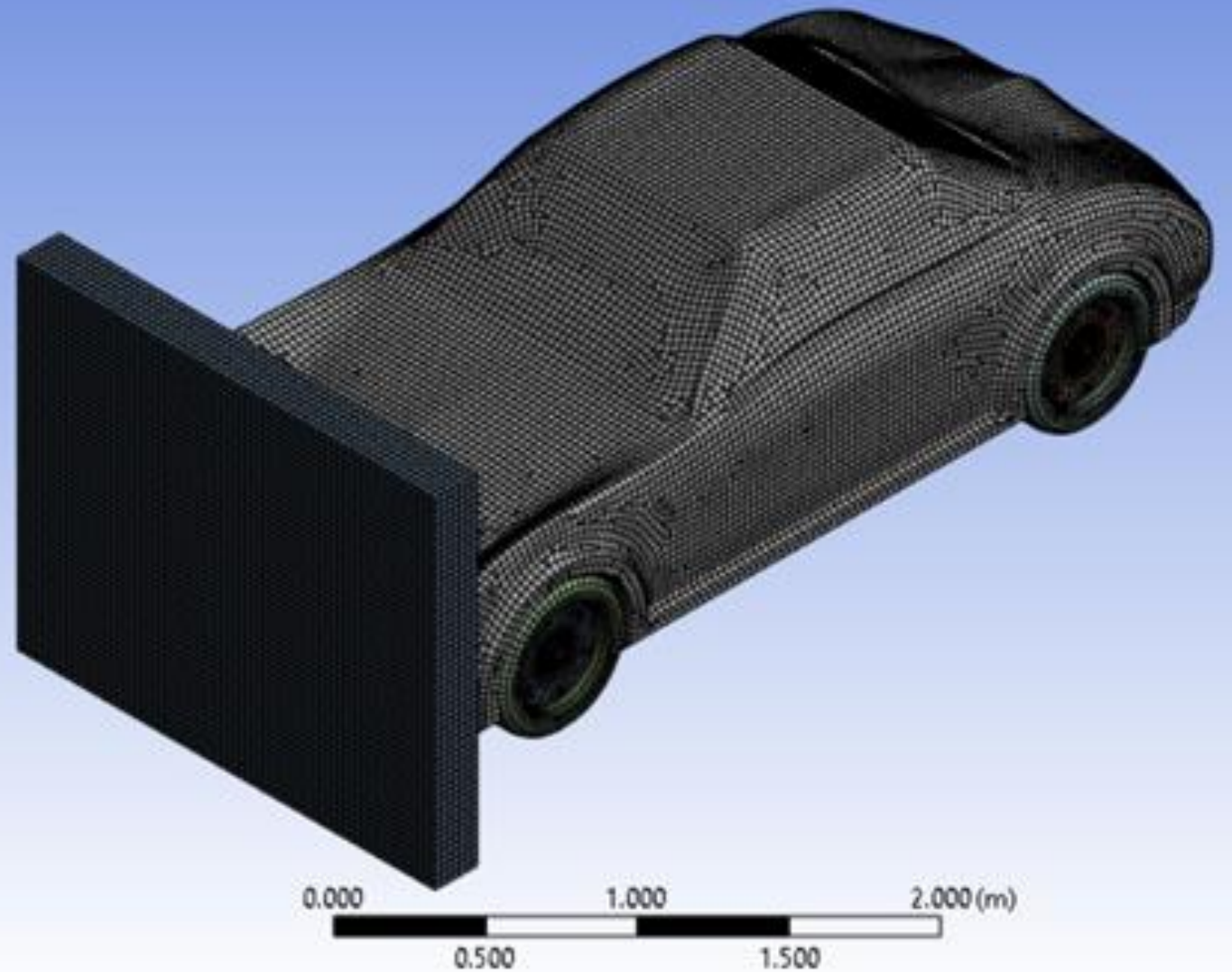


Click an object. Double-click to select an edge loop. Triple-click to select a solid.



PRE-PROCESSING

Preparing the model for the numerical simulation.

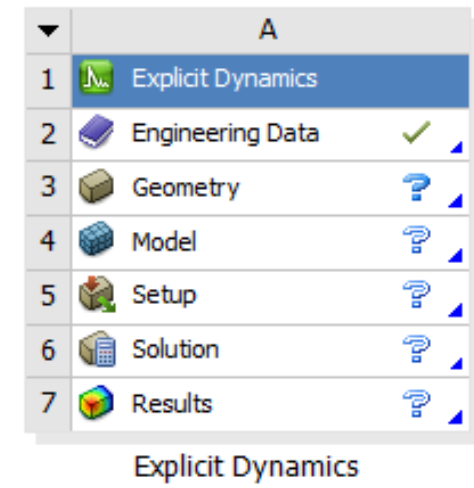

































PRE-PROCESSING: ENGINEERING DATA

Pre-processing in the context of solving a numerical method in ANSYS refers to the initial steps involved in setting up the problem and preparing the model for the numerical simulation. The pre-processing phase typically includes the following key steps:

- Selection of Analysis.
- Engineering Data.
- Geometry.
- Model.
- Setup.

Project Schematic



Outline of Schematic A2, B2, C2, D2, E2, F2, G2, H2, I2: Engineering Data					
	A	B	C	D	E
1	Contents of Engineering Data			Source	Description
2	 Material				
3	 AL 7075-T6			 E	"Equation of State and Strength Properties of Selected Materials". Steinberg D.J. LLNL. Feb 1991
4	 Aluminum Alloy			 G	General aluminum alloy. Fatigue properties come from MIL-HDBK-5H, page 3-277.
5	 Carbon Fiber T700			 C	
6	 Concrete			 G	
7	 Rubber1			 E	Coefficients fitted to experimental data from Treloar, L.R.G., Stress strain data for vulcanized rubber under various types of deformation, Transactions of the Faraday Society, vol. 40, pp.59-70 (1944)
8	 Structural Steel			 G	Fatigue Data at zero mean stress comes from 1998 ASME BPV Code, Section 8, Div 2, Table 5 -110.1
9	 TI 6%AL4%V			 E	"Equation of State and Strength Properties of Selected Materials". Steinberg D.J. LLNL. Feb 1991
*	Click here to add a new material				

ENGINEERING DATA

- Pre-defined materials can be selected from the “Engineering Data Resources” (or) new materials can be defined by double clicking the “Engineering Data” toolbar in Explicit dynamics module of ANSYS. Material properties are defined from the data mentioned in the chapter of methodology, with subcase 3.3.

Mechanical Properties of Materials

PROPERTIES	AL 7075T6	Ti-6Al-4V	CFRP T700 FIBER	Carbon Steel
Density (kg/m ³)	2810	4410	1800	7870
Specific Heat (J/kg-C)	870	526.3	752	472
Poisson's Ratio	0.33	0.342	0.3	0.29
Young's Modulus (GPa)	71.7	113.8	132	200
Yield Strength (MPa)	503	880	1450	415
Ultimate Tensile Strength (MPa)	572	950	2860	540
Strength-to-Weight Ratio (kN-m/kg)	203.56	215.42	1588.89	68.61
Percentage Elongation	11%	14%	2.02%	10%

Johnson Cook parameters of Materials

JC Parameters	AL 7075-T6	Ti-6Al-4V	CFRP T700 FIBER
Initial Yield Stress (A) – MPa	546	1098	67.2
Hardening Constant(B) – MPa	678	1092	100
Hardening Exponent(n)	0.71	0.93	0.046
Strain Rate Constant(C)	0.024	0.014	1.56
Thermal Softening Exponent(m)	1.56	1.1	1
Melting Temperature – °C	620	1605	3657
Reference Strain Rate - /sec	0.0005	1	0.00001

PRE-PROCESSING: ENGINEERING DATA

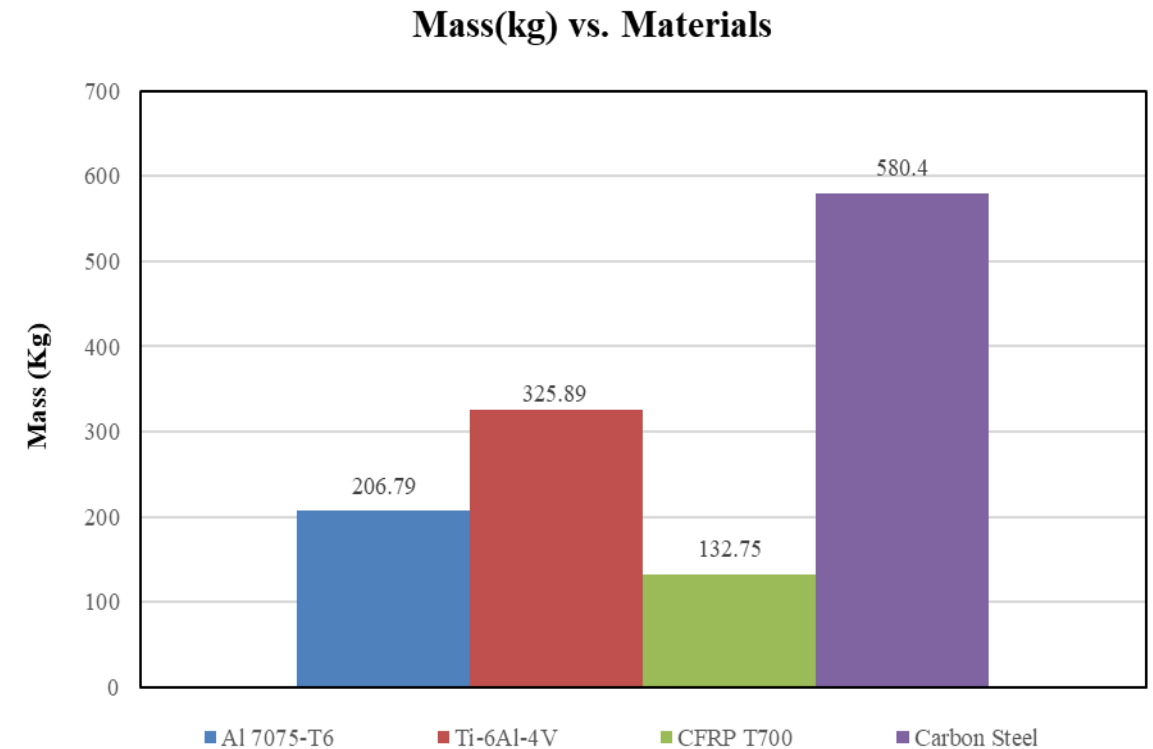
As there exists different geometries in the CAD model, each geometry should be assigned to its own material. Material assignment for different geometries are given below.

GEOMETRY	MATERIAL ASSIGNMENT	QUANTITY
RIGID BARRIER IMPACT TEST		
Car Body	Al 7075-T6	1 N
	Ti-6Al-4V	1 N
	CFRP T700	1 N
Tyre	Rubber 1	4 N
Rim	Aluminium alloy	4 N
Rigid Barrier – Frontal impact (Rectangle)	Concrete	1 N
Rigid Barrier – Side (pole) impact (Cylinder)		1 N
Rigid Barrier – Rollover impact (Rectangle)		1 N
CAR – TO – CAR IMPACT TEST		
Car Body	Al 7075-T6	2 N
	Ti-6Al-4V	2 N
	CFRP T700	2 N

PRE-PROCESSING: ENGINEERING DATA

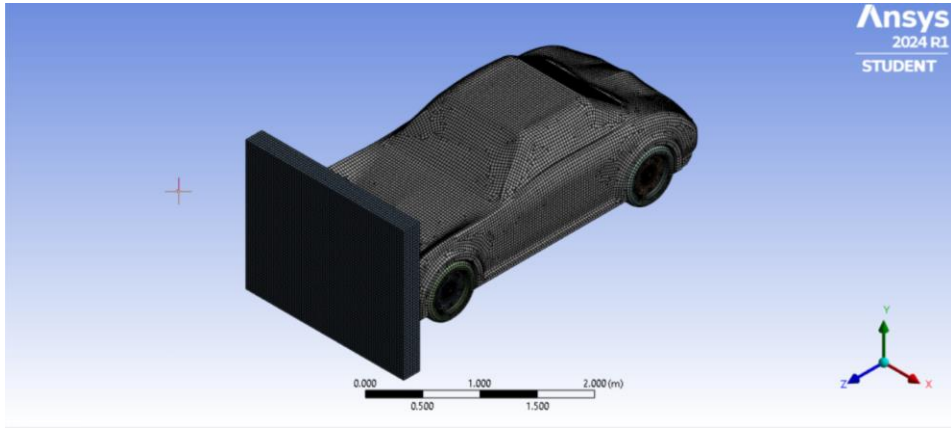
After assigning the material to the car body, for a 3mm of thickness, these are results obtained:

- Among the materials, the Carbon Steel has the highest weight at 580.4 kg for the car body designed in this project.
- CFRP T700 (132.75 Kg) has the highest weight reduction compared to carbon steel, at 77.1%. This indicates that CFRP T700 has the most favourable weight-to-strength ratio among the three lightweight materials.
- Al 7075-T6 (206.79 Kg) has the second-highest weight reduction at 64.4%, which is still significantly lower than the weight of carbon steel.
- Ti-6Al-4V (325.89 Kg) has the lowest weight reduction at 43.8% compared to carbon steel, but it still has a substantially lower weight than carbon steel.

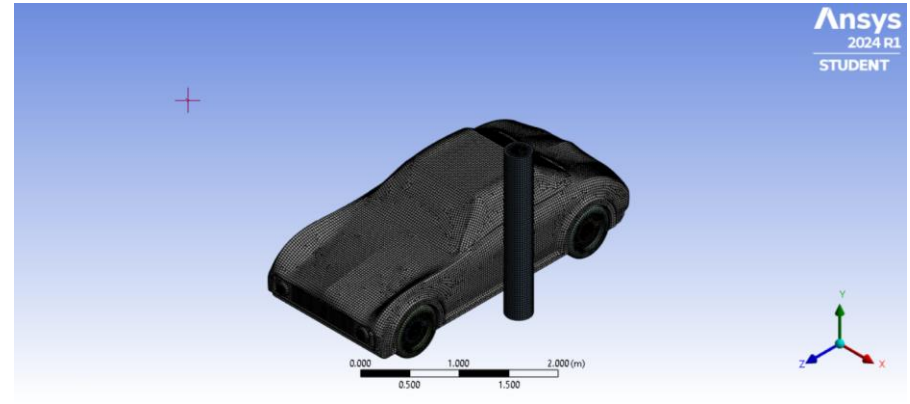


PRE-PROCESSING: MESHING

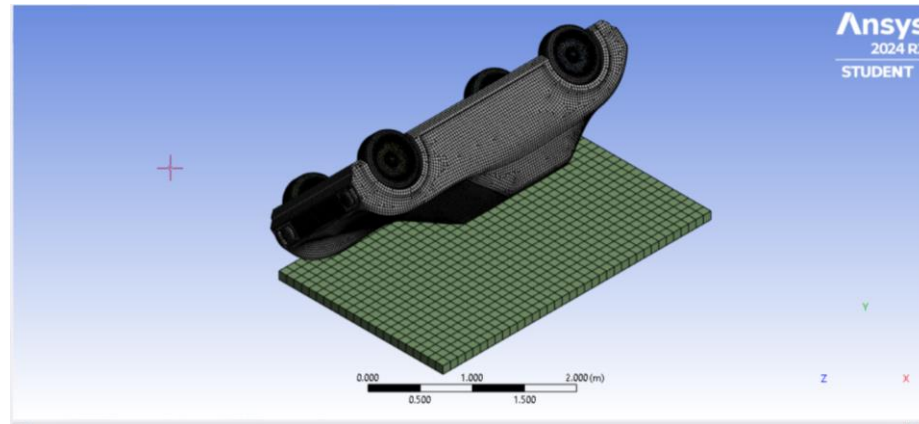
- Element metrics used in this project are: Triangle, quadrilateral, tetrahedra, hexagonal, and weighted edge discontinuity.
- Meshing with element size 28.784 mm. Maximum limit of elements: 1,28,000.



Elements: 91,532



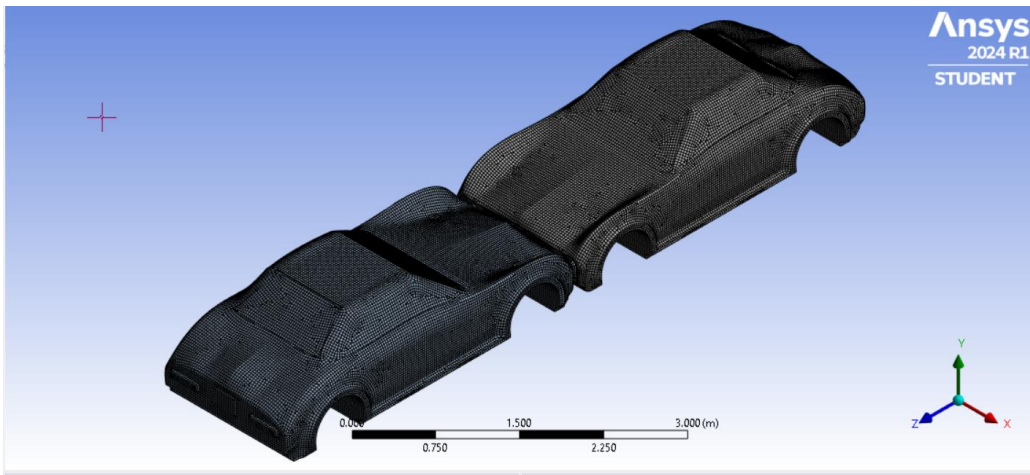
Elements: 94,231



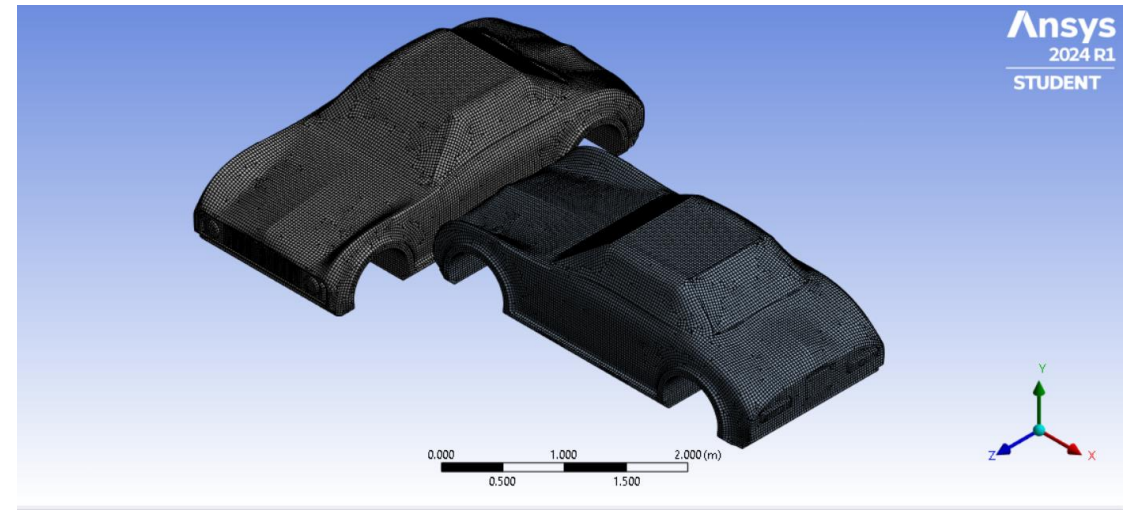
Elements: 96,389

PRE-PROCESSING: MESHING

- Meshing with element size 25.798 mm. Maximum limit of elements:1,28,000.



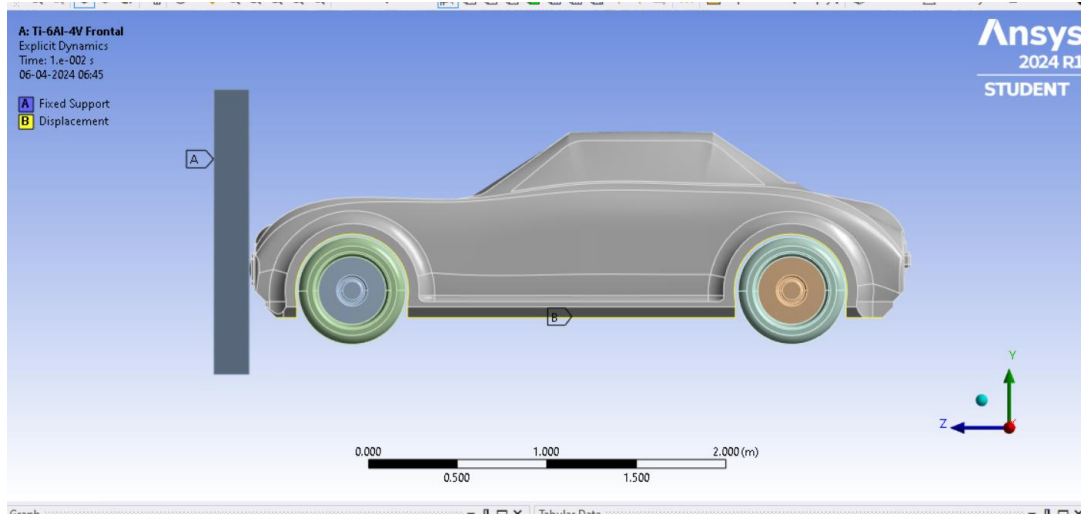
Elements: 82,482



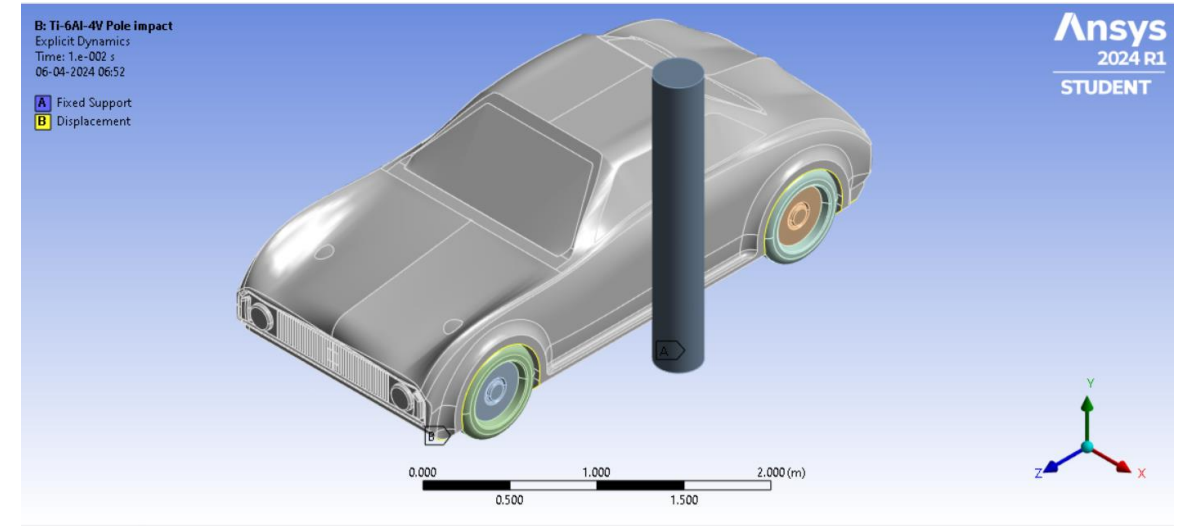
Elements: 82,482

PRE-PROCESSING: SETUP

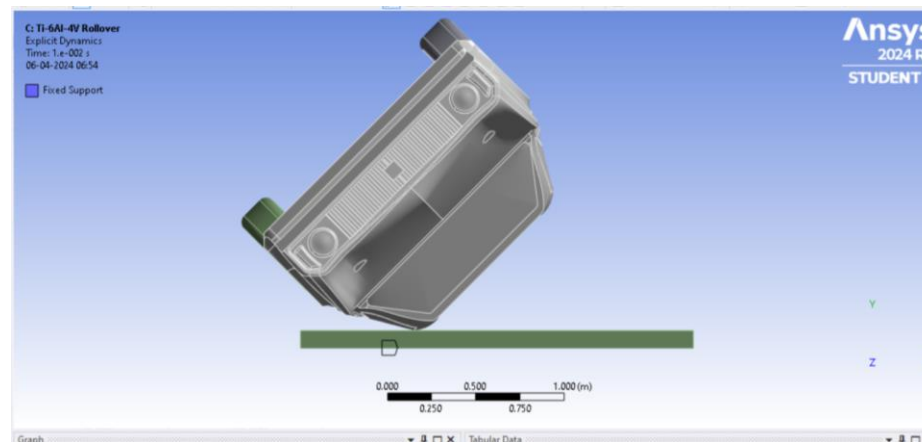
- **Setup:** Rigid Barrier is Fixed. Displacement of the lower car body edges is restricted. End time = 0.01 sec.



Velocity in Z: 80 m/s



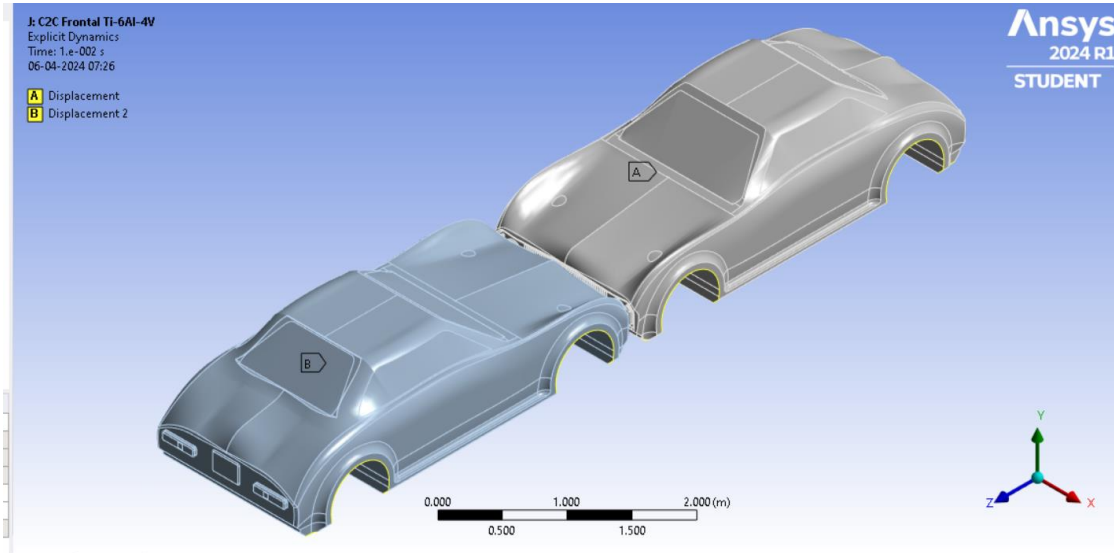
Velocity in X: 50 m/s



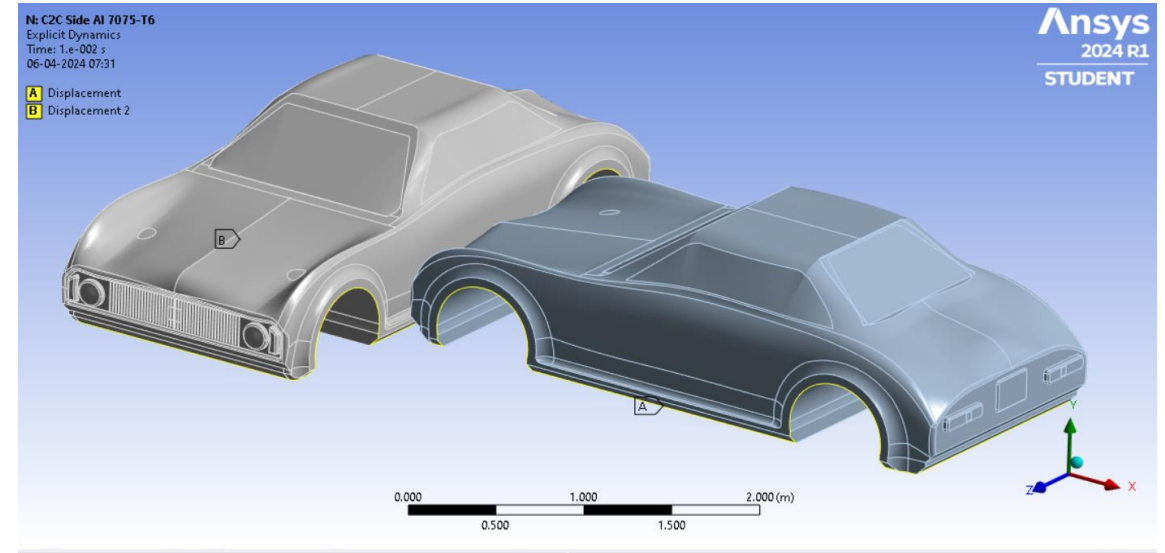
Velocity in X: 10 m/s
Velocity in Y: -30 m/s
Resultant velocity: 36.0555 m/s

PRE-PROCESSING: SETUP

- Setup: End time = 0.01 sec.



Velocity for Body(A): 100 m/s in Z -axis
Velocity for Body(B): -20 m/s in Z-axis



Velocity for Body(A): -100 m/s in X -axis
Velocity for Body(B): 20 m/s in Z-axis

SOLVING

- Solution Information:

Cycle: 178263, Time: 9.999E-03s, Time Inc.: 5.440E-08s, Progress: 99.99%, Est. Clock Time Remaining: 1s
Cycle: 178264, Time: 9.999E-03s, Time Inc.: 5.440E-08s, Progress: 99.99%, Est. Clock Time Remaining: 1s
Cycle: 178265, Time: 9.999E-03s, Time Inc.: 5.440E-08s, Progress: 99.99%, Est. Clock Time Remaining: 1s
Cycle: 178266, Time: 9.999E-03s, Time Inc.: 5.440E-08s, Progress: 99.99%, Est. Clock Time Remaining: 1s
Cycle: 178267, Time: 9.999E-03s, Time Inc.: 5.440E-08s, Progress: 99.99%, Est. Clock Time Remaining: 1s
Cycle: 178268, Time: 1.000E-02s, Time Inc.: 5.440E-08s, Progress: 100.00%, Est. Clock Time Remaining: 1s
Cycle: 178269, Time: 1.000E-02s, Time Inc.: 5.440E-08s, Progress: 100.00%, Est. Clock Time Remaining: 0s
Cycle: 178270, Time: 1.000E-02s, Time Inc.: 5.440E-08s, Progress: 100.00%, Est. Clock Time Remaining: 0s
Cycle: 178271, Time: 1.000E-02s, Time Inc.: 5.440E-08s, Progress: 100.00%, Est. Clock Time Remaining: 0s
Cycle: 178272, Time: 1.000E-02s, Time Inc.: 5.440E-08s, Progress: 100.00%, Est. Clock Time Remaining: 0s
Cycle: 178273, Time: 1.000E-02s, Time Inc.: 5.440E-08s, Progress: 100.00%, Est. Clock Time Remaining: 0s
Cycle: 178274, Time: 1.000E-02s, Time Inc.: 5.440E-08s, Progress: 100.00%, Est. Clock Time Remaining: 0s
Cycle: 178275, Time: 1.000E-02s, Time Inc.: 5.440E-08s, Progress: 100.00%, Est. Clock Time Remaining: 0s
Cycle: 178276, Time: 1.000E-02s, Time Inc.: 5.440E-08s, Progress: 100.00%, Est. Clock Time Remaining: 0s
Cycle: 178277, Time: 1.000E-02s, Time Inc.: 5.440E-08s, Progress: 100.00%, Est. Clock Time Remaining: -

SIMULATION ELAPSED TIME SUMMARY

EXECUTION FROM CYCLE 0 TO 178277
ELAPSED RUN TIME IN SOLVER = 3.56912E+02 Minutes
TOTAL ELAPSED RUN TIME = 3.59616E+02 Minutes
JOB RAN OVER 4 WORKERS
JOB RAN USING Intel MPI
JOB RAN USING DECOMPOSITION AUTO

Problem terminated wrapup time reached

- End Time = Cycles x Time Increment

Comparison of solving time for the tests w.r.t processors used for simulation

TEST CODE	NO. OF CYCLES	TIME INCREMENTS	END TIME	PROCESSOR USED	SOLVING TIME
Test1	163935	9.701E-08s	0.01 s	11 th Gen Intel® i5-11260H @ 2.60GHz	2.12936E+02 Minutes
Test2	165644	6.039E-08s	0.01 s	11 th Gen Intel® i5-11260H @ 2.60GHz	2.12176E+02 Minutes
Test3	165770	6.018E-08s	0.01 s	11 th Gen Intel® i5-11260H @ 2.60GHz	2.72897E+02 Minutes
Test4	178277	5.440E-08s	0.01 s	Intel® Xeon® W-2123 CPU @ 3.60GHz	3.59616E+02 Minutes
Test5	174964	5.582E-08s	0.01 s	Intel® Xeon® W-2123 CPU @ 3.60GHz	3.55369E+02 Minutes

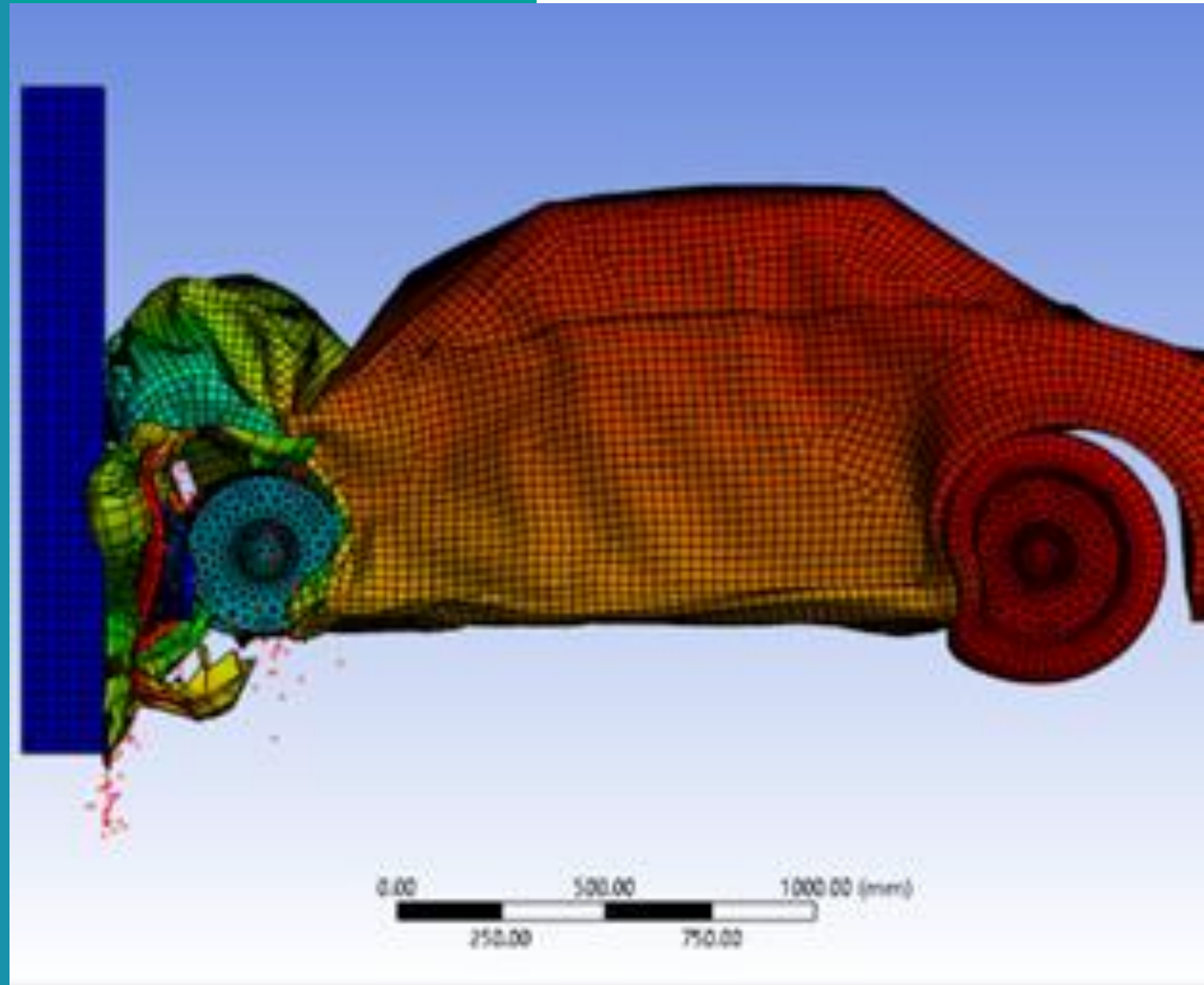
Each test has 3 subcases present in it i.e., conducting crash test analysis for 3 different lightweight materials: Al 7075-T6, Ti-6Al-4V, and CFRP T700. By calculating, the solving time for each subcase of a test, we get:

- Total solving time for test-1 = 638.808 minutes = 10.6468 hrs.
- Total solving time for test-2 = 636.528 minutes = 10.6088 hrs.
- Total solving time for test-3 = 818.691 minutes = 13.64485 hrs.
- Total solving time for test-4 = 1,078.848 minutes = 17.9808 hrs.
- Total solving time for test-5 = 1,066.107 minutes = 17.76845 hrs.

Therefore, the total time took by the solver AUTODYN to solve the 15 mathematical models for car crash test is **70.6497 hours**.

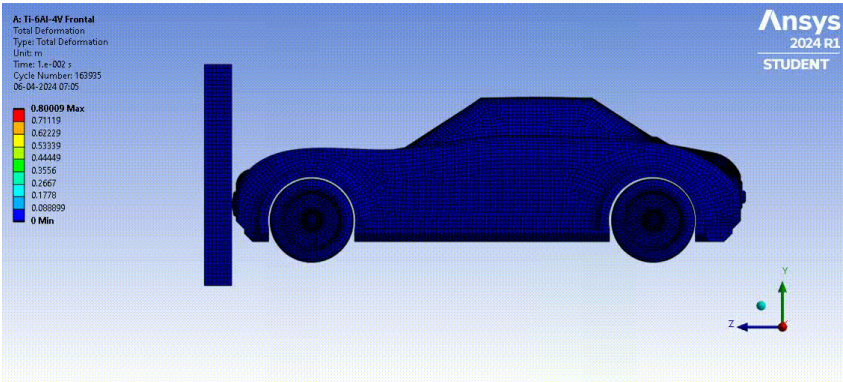
POST – PROCESSING

Evaluating the results from the
solved mathematical model.



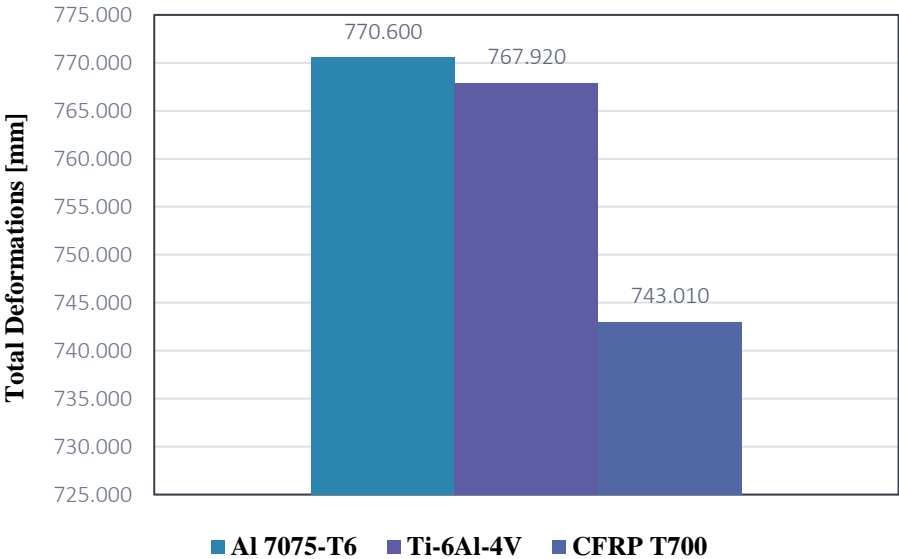
POST-PROCESSING: DEFORMATIONS

- Deformations: TEST-1



Time[s]	Deformations for Al 7075-T6[mm]	Deformations for Ti-6Al-4V[mm]	Deformations for CFRP T700[mm]
1.18E-38	0.000	0.000	0.000
2.50E-03	204.160	204.380	240.210
5.00E-03	402.650	401.650	429.190
7.50E-03	592.220	592.720	569.100
1.00E-02	770.600	767.920	743.010

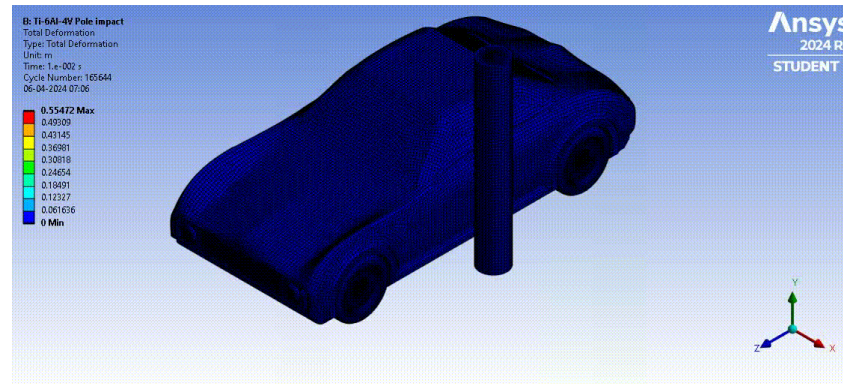
Total Deformation [mm] vs. Materials



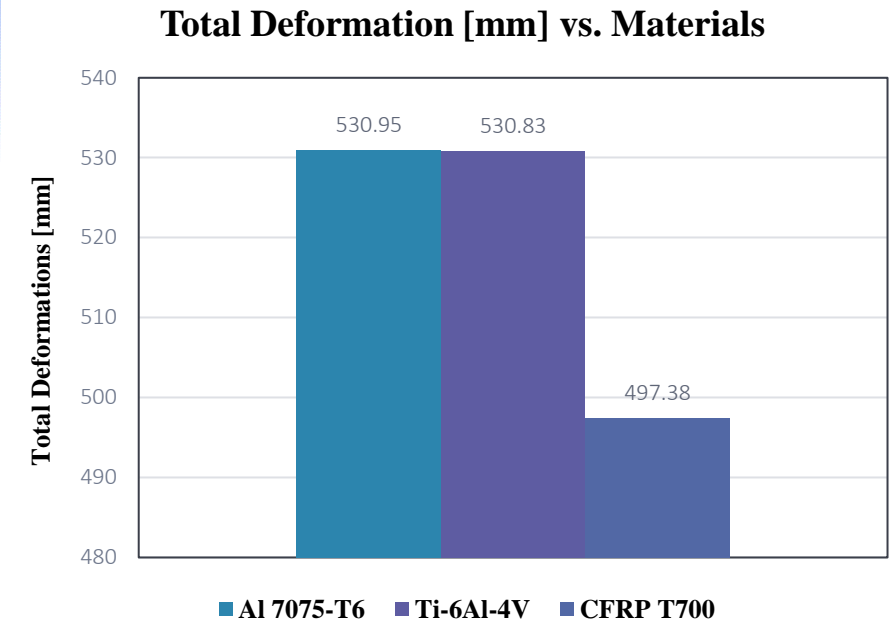
By evaluating the total deformation command, the test-1 results can be observed as the lightweight material CFRP T700 tends to deform less than the other lightweight materials Al 7075-T6, Ti-6Al-4V. Car body assigned with CFRP T700 fiber undergoes 743.010 mm of deformation; body assigned with Ti-6Al-4V alloy undergoes 767.920 mm of deformation; and body assigned Al 7075-T6 alloy undergoes 770.6 mm of deformation.

POST-PROCESSING: DEFORMATIONS

- Deformations: TEST2



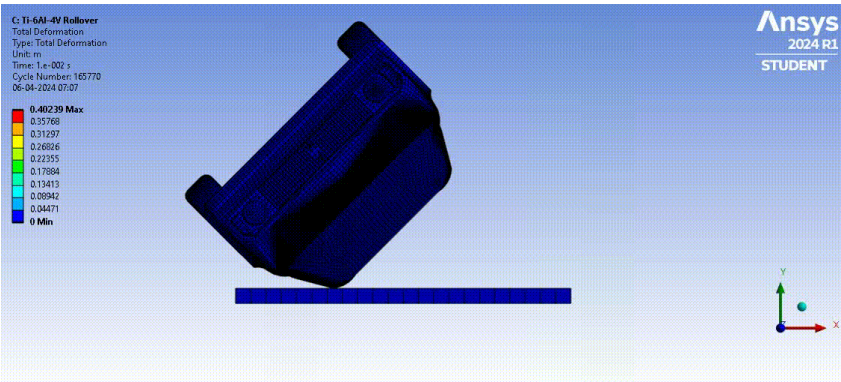
Time[s]	Deformations for Al 7075-T6 [mm]	Deformations for Ti-6Al-4V [mm]	Deformations for CFRP T700 [mm]
1.18E-38	0	0	0
2.50E-03	142.89	143.5	156.32
5.00E-03	277.2	278.88	262.18
7.50E-03	394.9	395.41	380.81
1.00E-02	530.95	530.83	497.38



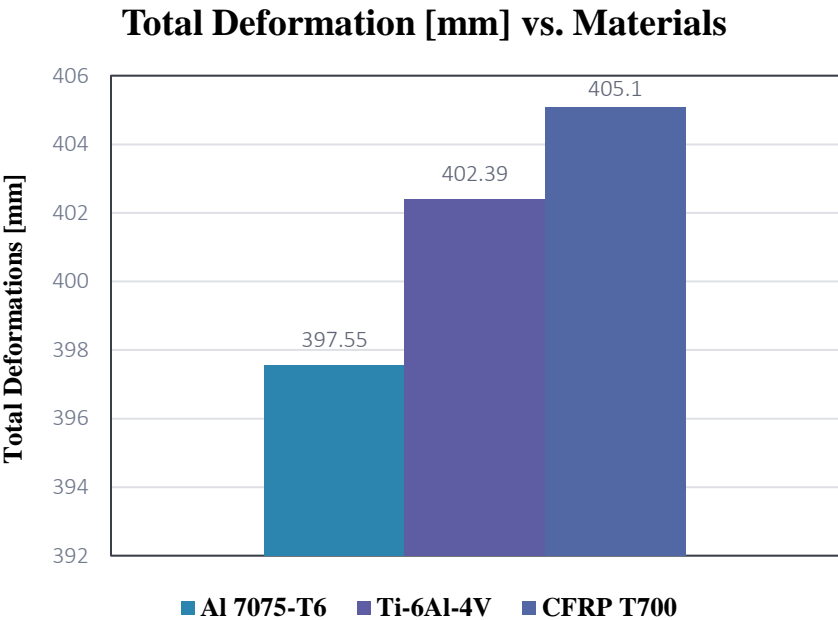
By evaluating the total deformation command, the test-2 results can be observed as the lightweight material CFRP T700 tends to deform less than the other lightweight materials Al 7075-T6, Ti-6Al-4V. Car body assigned with CFRP T700 fiber undergoes 497.38 mm of deformation; body assigned with Ti-6Al-4V alloy undergoes 530.83 mm of deformation; and body assigned Al 7075-T6 alloy undergoes 530.95 mm of deformation.

POST-PROCESSING: DEFORMATIONS

- Deformations: TEST3



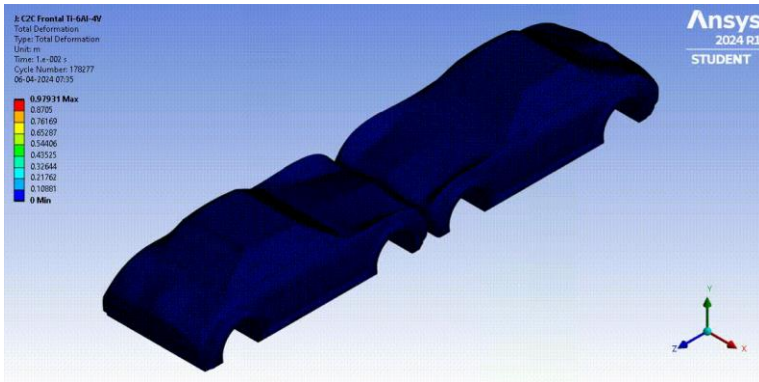
Time[s]	Deformations for Al 7075-T6[mm]	Deformations for Ti-6Al-4V[mm]	Deformations for CFRP T700[mm]
1.18E-38	0	0	0
2.50E-03	115.5	116.47	119.49
5.00E-03	204.7	207.88	212.52
7.50E-03	294.07	297.35	305.36
1.00E-02	397.55	402.39	405.1



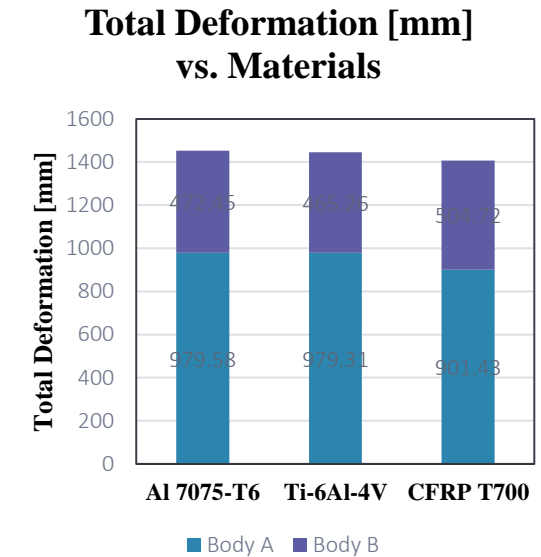
By evaluating the total deformation command, the test-3 results can be observed as the lightweight material Al 7075-T6 tends to deform less than the other lightweight materials CFRP T700, Ti-6Al-4V. Car body assigned with Al 7075-T6 alloy undergoes 397.55 mm of deformation; body assigned with Ti-6Al-4V alloy undergoes 402.39 mm of deformation; and body assigned CFRP T700 fiber undergoes 530.95 mm of deformation.

POST-PROCESSING: DEFORMATIONS

- Deformations: Car-to-car Frontal analysis. (TEST4)



Time [s]	Deformations for Al 7075-T6 [mm]		Deformations for Ti-6Al-4V [mm]		Deformations for CFRP T700 [mm]	
	Body A	Body B	Body A	Body B	Body A	Body B
1.18E-38	0	0	0	0	0	0
2.50E-03	258.74	135.53	258.49	135.66	272.89	114.79
5.00E-03	501.79	238.59	501.6	242.68	506.99	239.38
7.50E-03	746.09	362.96	745.8	349.45	711.15	410.5
1.00E-02	979.58	472.45	979.31	465.26	901.43	504.72

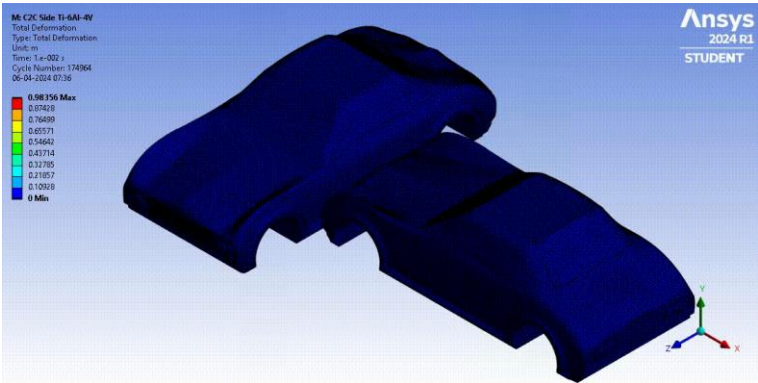


By evaluating the total deformation command, the test-4 results can be observed as the lightweight material CFRP T700 tends to deform less for car body A, than the other lightweight materials Al 7075-T6, Ti-6Al-4V. But the car body B which is moving with lower velocities undergoes high deformations while compared to other car bodies B of lightweight materials.

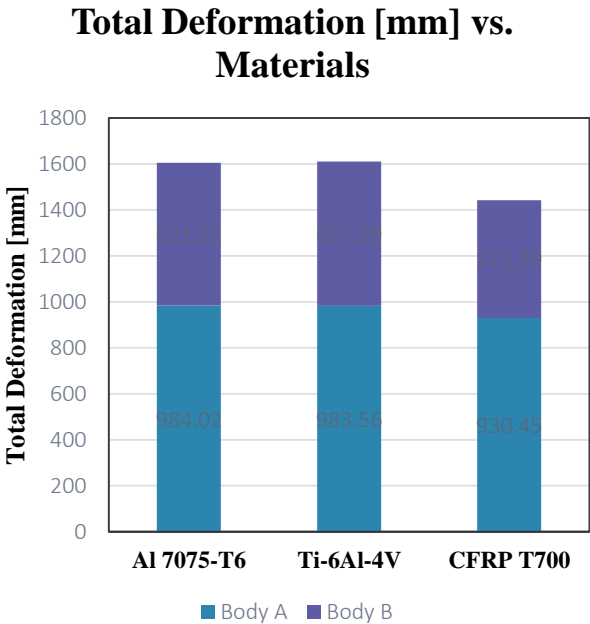
Considering overall deformations of two bodies, CFRP T700 undergoes less deformations, compared to other lightweight materials.

POST-PROCESSING: DEFORMATIONS

- Deformations: Car-to-car Side analysis. (TEST5)



Time [s]	Deformations for Al 7075-T6 [mm]		Deformations for Ti-6Al-4V [mm]		Deformations for CFRP T700 [mm]	
	Body A	Body B	Body A	Body B	Body A	Body B
1.18E-38	0	0	0	0	0	0
2.50E-03	256.27	178.07	256.28	178.42	256.63	155.34
5.00E-03	505.83	324.53	505.54	324.68	511.92	311.13
7.50E-03	751.58	478.95	747.97	478.96	720.76	419.33
1.00E-02	984.02	621.61	983.56	627.69	930.45	511.39



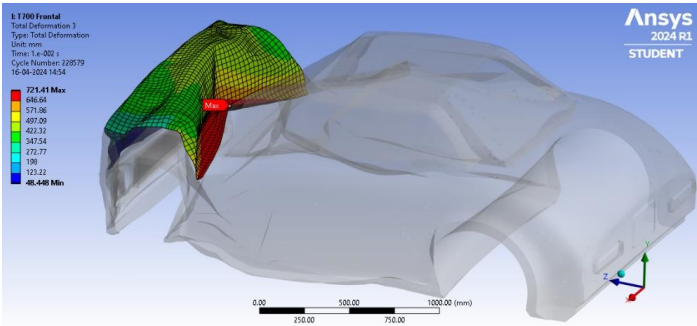
By evaluating the total deformation command, the test-5 results can be observed as the lightweight material CFRP T700 tends to deform less for car body A and body B too, than the other lightweight materials Al 7075-T6, Ti-6Al-4V. Considering overall deformations of two bodies, CFRP T700 undergoes less deformations, compared to other lightweight materials. And Ti-6Al-4V proves to be a better material that undergoes less deformations than Al 7075-T6 alloy.

POST-PROCESSING: DEFORMATIONS

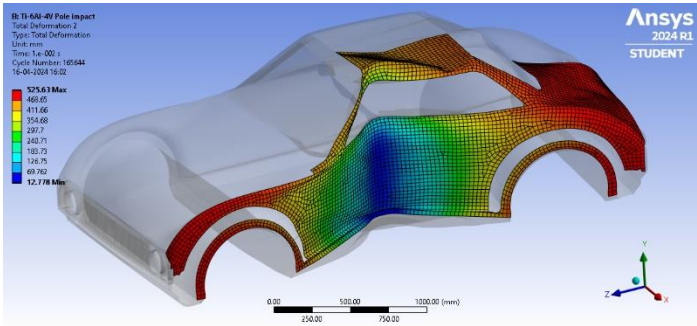
Deformations (mm)	Al 7075-T6	Ti-6Al-4V	CFRP T700
RIGID BARRIER ANALYSES			
Frontal Impact	770.6	767.92	743.01
Side (Pole) Impact	530.95	530.83	497.38
Rollover Impact	397.55	402.39	405.1
CAR-TO-CAR ANALYSES			
Frontal Impact	979.58	979.31	901.43
Side Impact	984.02	983.56	899.5

POST-PROCESSING: MAXIMUM DEFORMATIONS

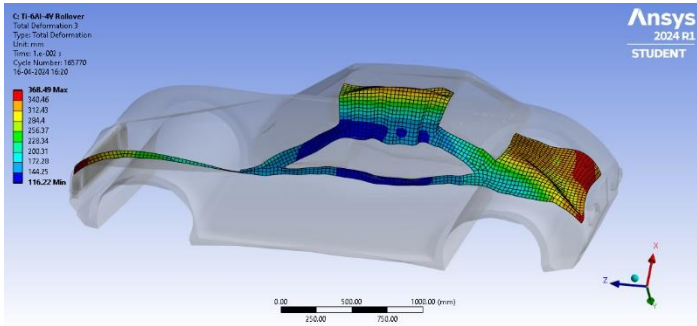
The parts: Bonnet, side door panels, and roof top panels of the car body undergoes the maximum deformations in the whole car body, for the frontal impact, side impact, and rollover impact barrier tests respectively, for the corresponding materials, CFRP T700, and Ti-6Al-4V.



Bonnet



Side Door Panels

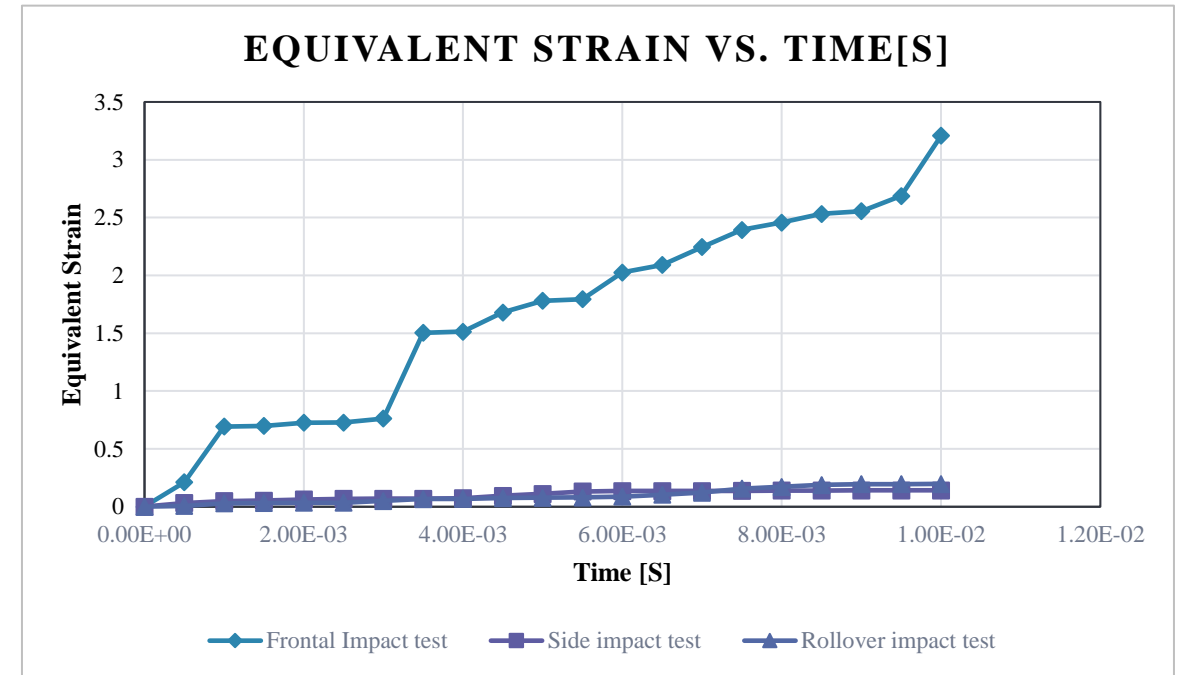
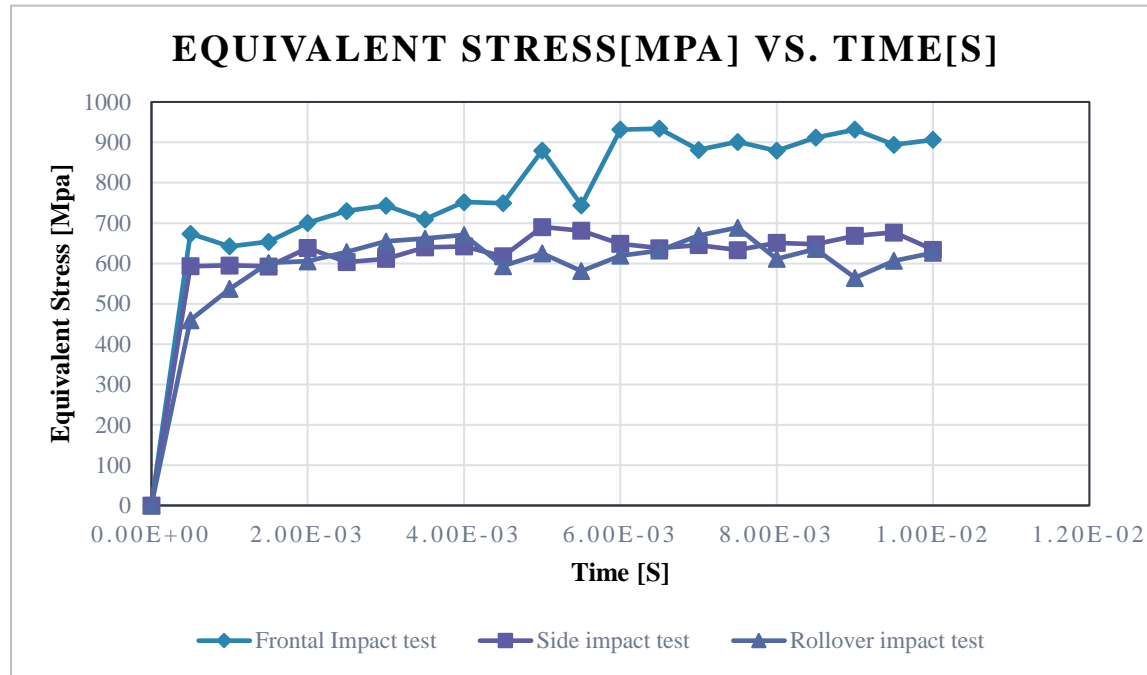


Roof top Panels

TEST CODE	MAXIMUM DEFORMED PART	MAXIMUM DEFORMED MATERIAL	MAXIMUM DEFORMATION [mm]
Test-1	Bonnet	CFRP T700	721.41
Test-2	Side door panels	Ti-6Al-4V	525.63
Test-3	Roof top panels	Ti-6Al-4V	368.49

POST-PROCESSING: Stress & Strain Analysis for Al 7075-T6

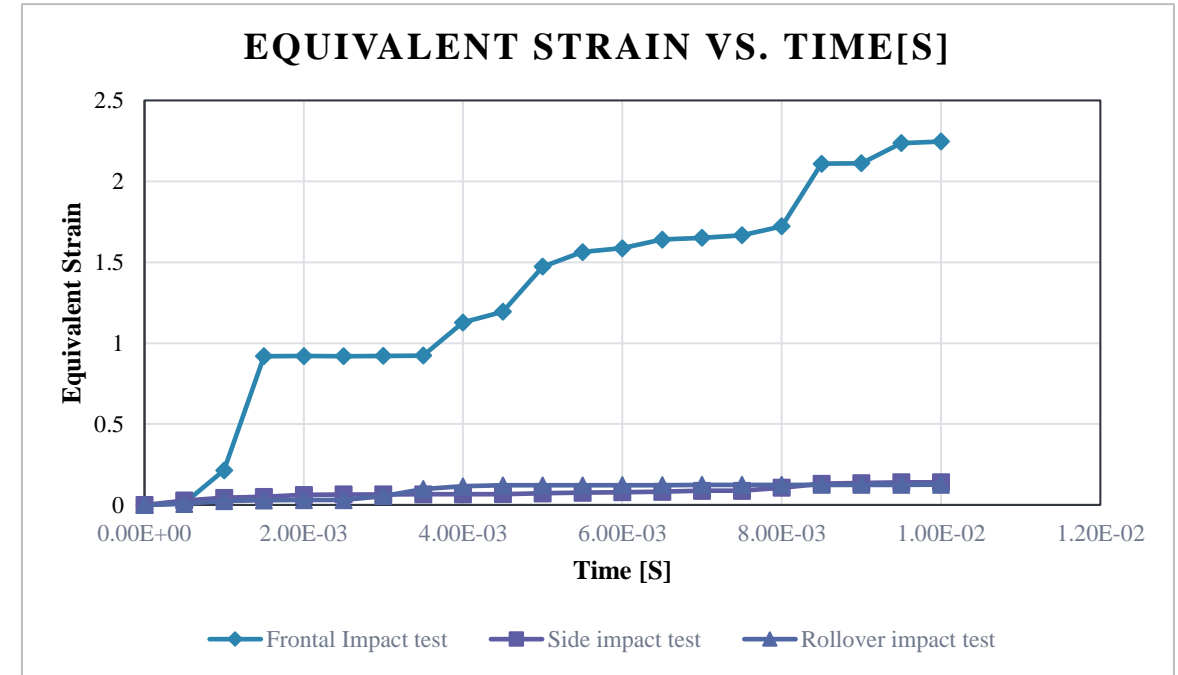
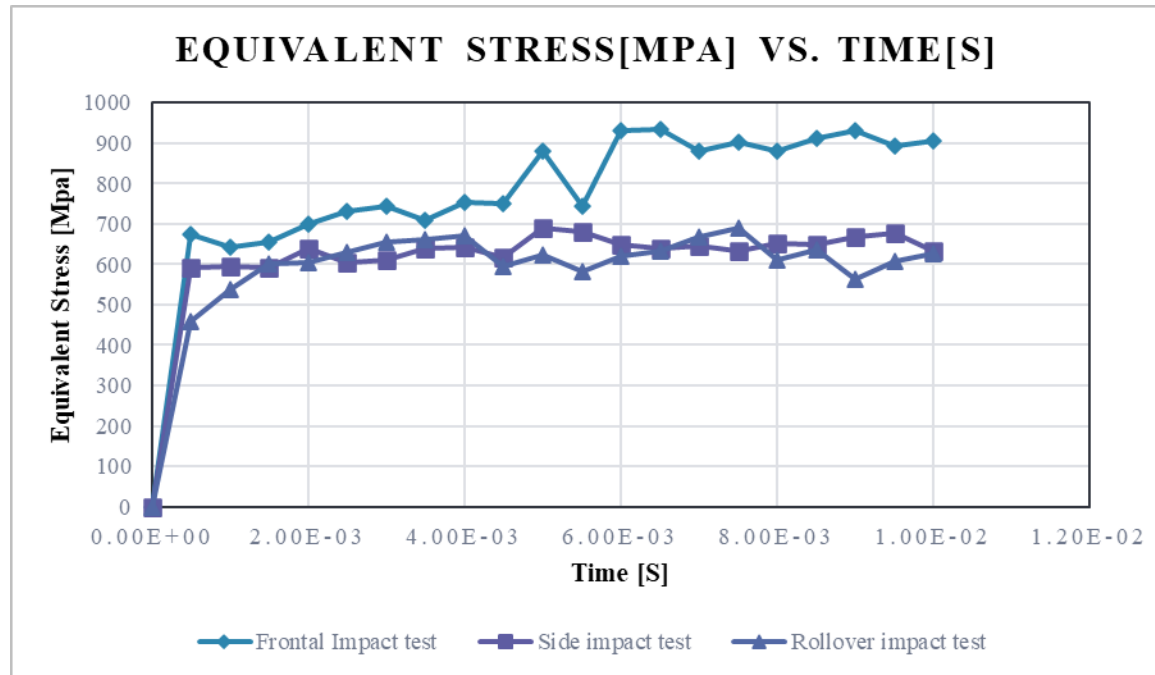
The maximum stresses developed by the car body with Al 7075-T6 alloy, upon impacting the rigid barriers by the end time are 906.32 MPa in frontal impact, 633.88 MPa in side (pole) impact, and 626.62 MPa in rollover impact test.



From the above two graphs, we can conclude that the stresses and strains developed in frontal barrier impact of the car body of Al 7075-T6 alloy, are higher than the other barrier impact tests.

POST-PROCESSING: Stress & Strain Analysis for Ti-6Al-4V

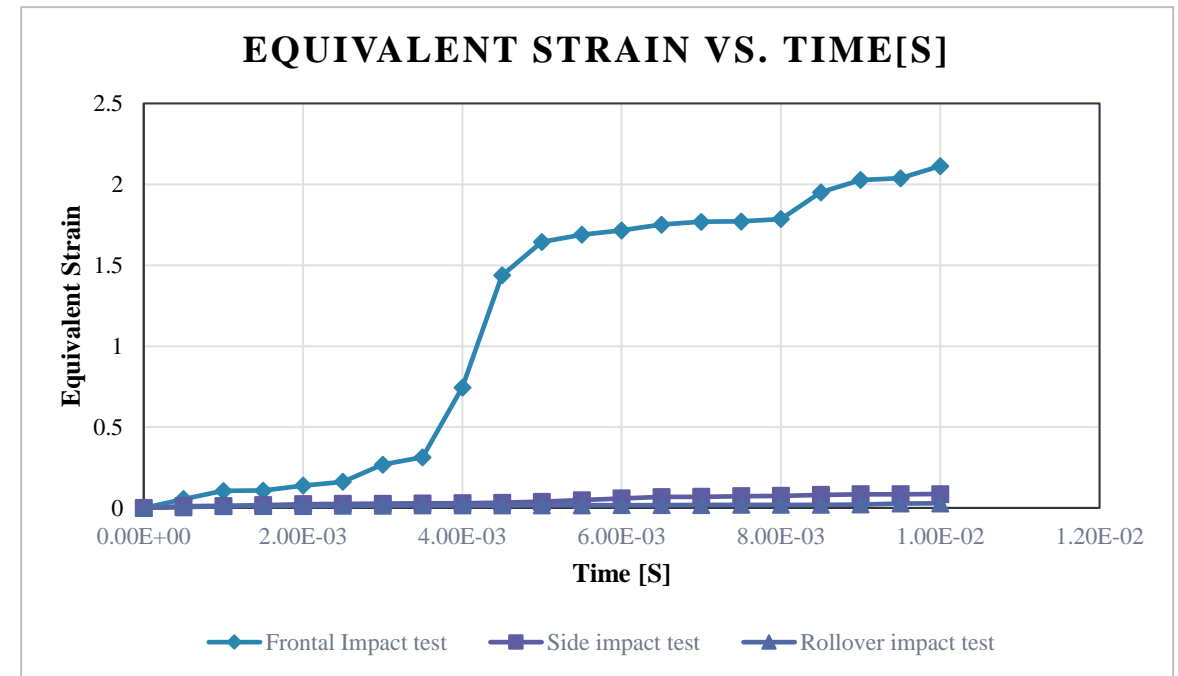
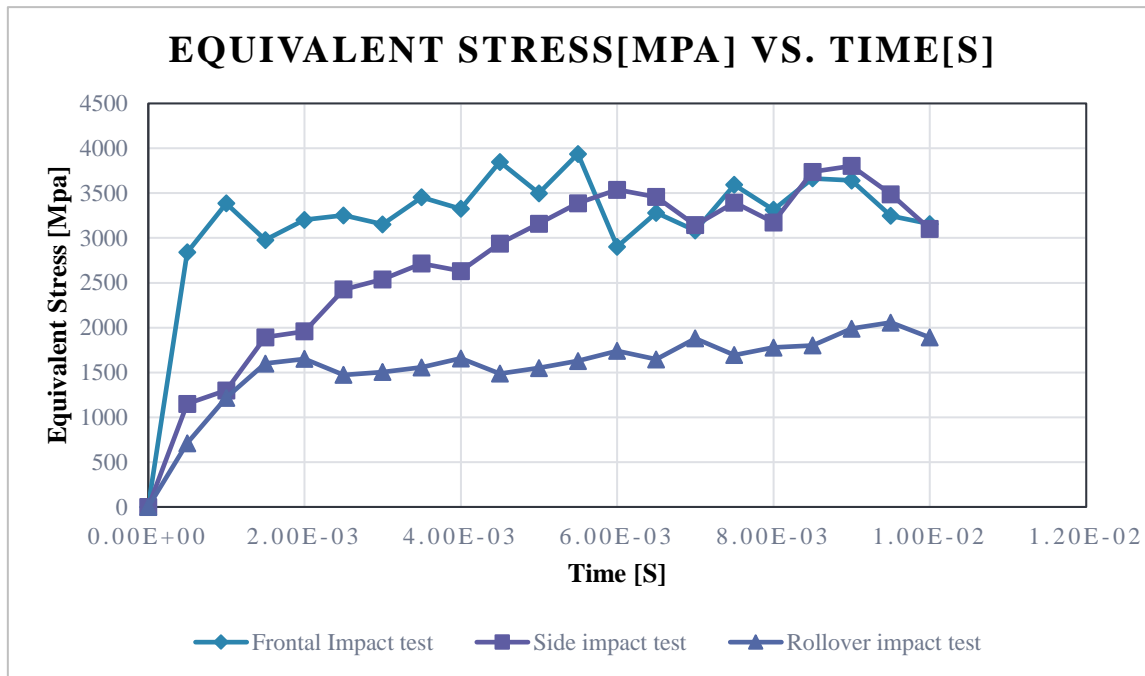
The maximum stresses developed by the car body with Ti-6Al-4V alloy, upon impacting the rigid barriers by the end time are 1306.2 MPa in frontal impact, 1238.8 MPa in side (pole) impact, and 1085.8 MPa in rollover impact test.



From the above two graphs, we can conclude that the stresses and strains developed in frontal barrier impact of the car body of Ti-6Al-4V alloy, are higher than the other barrier impact tests.

POST-PROCESSING: Stress & Strain Analysis for CFRP T700

The maximum stresses developed by the car body with CFRP T700 fiber, upon impacting the rigid barriers by the end time are 3155.3 MPa in frontal impact, 3100.9 MPa in side (pole) impact, and 1890.6 MPa in rollover impact test.



From the above two graphs, we can conclude that the stresses and strains developed in frontal barrier impact of the car body of CFRP T700, are higher than the other barrier impact tests.

POST-PROCESSING: Stress & Strain Analysis for CFRP T700

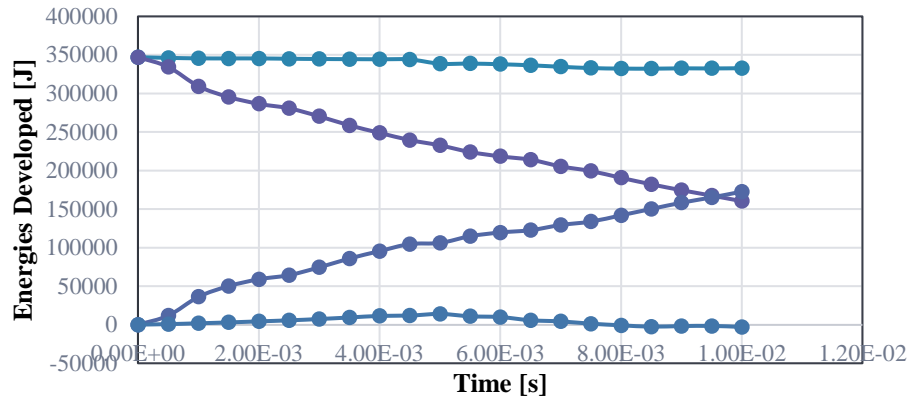
Comparison of stresses and strains induced in the car body for different materials

MATERIAL	TEST CODE	STRESSES [MPa]	STRAINS [mm/mm]
Al 7075-T6	Test-1	906.32	3.2093
	Test-2	633.88	0.140218
	Test-3	626.62	0.1954107
Ti-6Al-4V	Test-1	1306.2	2.24624
	Test-2	1238.8	0.140793
	Test-3	1085.8	0.125271
CFRP T700	Test-1	3155.3	2.11282
	Test-2	3100.9	0.085749
	Test-3	1890.6	0.0284339

From the above graphs and tables of stresses and strains induced in the body, we can conclude that the CFRP is resisting to the external load, a lot more greater than the other two materials.

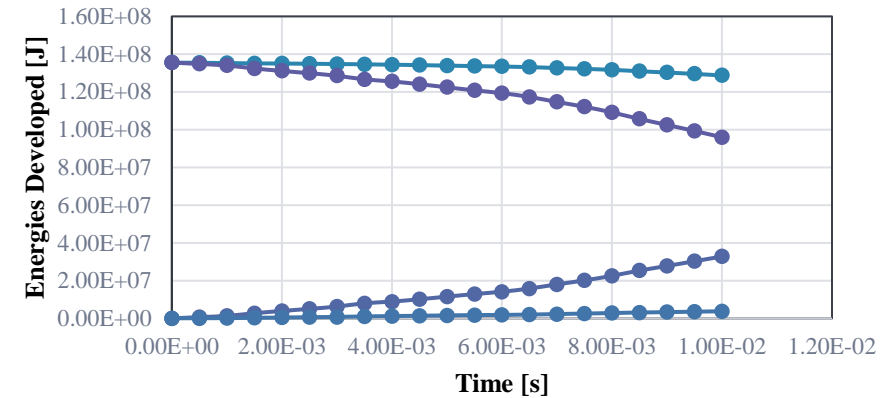
POST-PROCESSING: ENERGIES vs. TIME

ENERGY [J] vs. TIME [s]



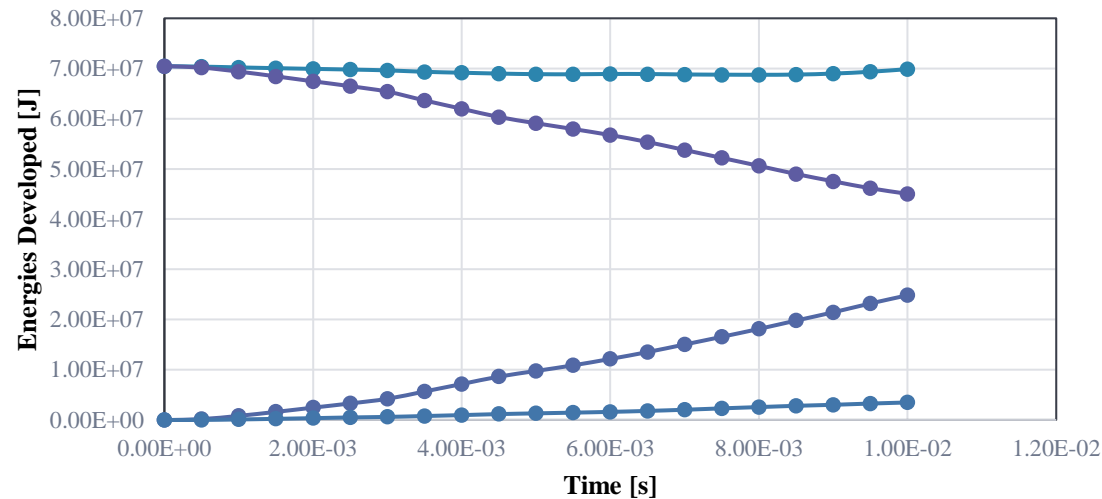
Frontal barrier
impact test

ENERGY [J] vs. TIME [s]



Side barrier
impact test

ENERGY [J] vs. TIME [s]



Rollover barrier
impact test

POST-PROCESSING: ENERGIES vs. TIME

From the obtained graphs of energies developed in a car body for car crash test to a rigid barrier, the kinetic energy of the car body obtained from initial velocity, is transformed into the internal energy and the hourglass energy.

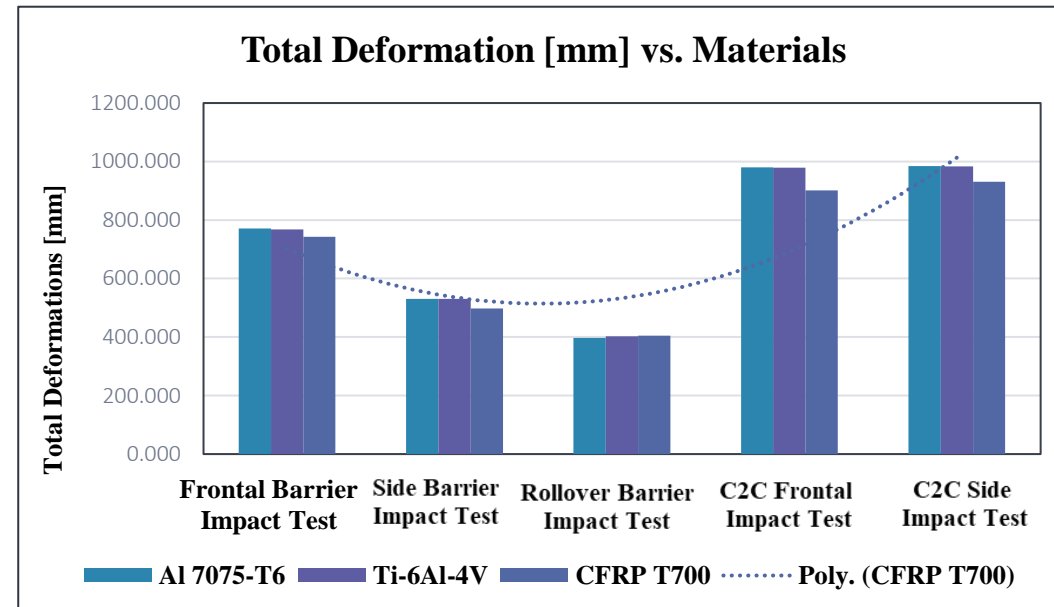
From these graphs we can conclude that the:

- 1) Total energy would remain constant.
- 2) Loss in kinetic energy will be transformed into internal energy, and hourglass energy.
- 3) Hourglass energy is less than 5% of internal energy, if it is not the case, proper hour glassing should be given to the material.

CONCLUSIONS

These are the conclusions obtained from the series of analyses conducted on the car body:

- From the below-mentioned graph, we can conclude that the deformations for the materials Al 7075-T6 and Ti-6Al-4V are almost same, but Ti-6Al-4V undergoes lower deformations than Al 7075-T6.
- However, in the case of rollover analyses, the Al 7075-T6 is proved to be an optimal material for the car body. CFRP T700 undergoes less deformations compared to other two materials except rollover analyses.
- However, in case of Car-to-car frontal analysis, the Car B tends to deform more than other materials, but including Body A & B, the overall deformations for CFRP T700 were lower than the other materials in frontal crash of Car-to-car analysis.



CONCLUSIONS

- Overall, the CFRP T700 fiber proves to be the best material for a car body that can undergo less deformations under high speeds, within these selected materials, except the rollover analyses.
- The parts: Bonnet, side door panels, and roof top panels of the car body undergoes the maximum deformations in the whole car body, for the frontal impact, side impact, and rollover impact barrier tests respectively, for the corresponding materials, CFRP T700, and Ti-6Al-4V.
- From the stress and strain analyses too, CFRP resists to the external loads better than other two materials and allowing the material to change its original dimensions, less. However, Ti-6Al-4V alloy performs better than Al 7075-T6 alloy, in the case of stresses and strains induced in the body.
- From the analyzing the energies developed in the car body, it is concluded that, loss in kinetic energy will be transformed into internal energy, and hourglass energy. And Total energy would remain constant.

At last, it is concluded that the best material for the car body would be the CFRP T700 fiber. However, for the roof top body part, it can be replaced by the Al 7075-T6 alloy, as it undergoes low deformations compared to other two materials in rollover analysis. Rollover analysis was a special case, where the materials of high stiffnesses undergo high deformations. However, in all other crash tests, CFRP T700 fiber undergoes low deformations and strains, and high stresses, and comparatively Ti-6Al-4V alloy performs better than Al 7075-T6 alloy.

COST ANALYSIS

COST COMPONENT	DESCRIPTION	EXPENDITURE COST(INR)
Software License	ANSYS software Student license for crash simulations	Rs. 0/-
CAD Model Development	Cost for creating and refining car CAD model	Rs. 0/-
Material Acquisition	Expenses for purchasing different types of materials (Included within the ANSYS software student version)	Rs. 0/-
Computing Resources	Cost for high-performance computing for simulations (Owned Laptops)	Rs. 0/-
Expertise/Consulting Fees	Guidance from experienced consultants/ Engineers (MayinKrish Ventures Pvt. Ltd.)	Rs. 7,000/-
Training and Education	Specialized ANSYS crash analysis training (MayinKrish Ventures Pvt. Ltd.)	Rs. 3,000/-
TOTAL COST		Rs. 10,000/-

REFERENCES



- 1) Sun, H., Shen, G., & Hu, P. (2009). Study on Lightweight Optimization of Car Body Based on Crash. Journal of Automotive Engineering, 2009(5), 72-80. <https://doi.org/10.1109/ICICTA.2009.459>.
- 2) Tejasagar, A., Srikanth, K. V. N. S., & Veeraraju, P. (2012). Simulation of Frontal Crash Tests Using LS-DYNA Software. International Journal of Crashworthiness, 17(6), 649-658. <http://dx.doi.org/10.13140/RG.2.2.11183.38560>.
- 3) Babu, T. A., Praveen, D. V., & Venkateswarao, M. (2012). Crash Analysis of Car Chassis Frame Using Finite Element Method. International Journal of Vehicle Structures & Systems, 4(2), 67-74.
- 4) Johannsen, H., et al. (2012). Vehicle Safety in Frontal Collisions: Frontal Impact and Compatibility Assessment Research: How to test self and partner protection. International Journal of Crashworthiness, 17(4), 391-399. <https://doi.org/10.1016/j.sbspro.2012.06.1233>.
- 5) Zhu, Y., Li, L., & Yang, J. (2012). Frontal Structure Improvement on Car Based on RCAR Impact Test. Journal of Automotive Safety and Energy, 3(2), 123-134. <https://doi.org/10.1109/ICDMA.2012.104>.
- 6) Li, G., & Yang, J. (2012). Influence of Vehicle Front Structure on Car-to-SUV Crash Compatibility. Journal of Vehicle Engineering, 12(3), 212-223. <https://doi.org/10.1109/ICDMA.2012.117>.
- 7) Biqiang, Z., Shugang, X., & Rui, F. (2013). Study on the Response of the Car Crash by Move Distorted Barrier. Journal of Automotive Safety and Compliance, 4(1), 45-56. <https://doi.org/10.1109/ICMTMA.2013.270>.

- 8) Wang, X., & Shi, J. (2013). Validation of Johnson-Cook Plasticity and Damage Model using Impact Experiment. *Materials Science and Engineering*, 23(5), 890-899. <https://doi.org/10.1016/j.ijimpeng.2013.04.010>.
- 9) Liu, C., Song, X., & Wang, J. (2014). Simulation Analysis of Car Front Collision Based on LS-DYNA and Hyper Work. *International Journal of Vehicle Crashworthiness*, 19(3), 298-307. <http://dx.doi.org/10.4236/jtts.2014.44030>.
- 10) Lokhande, A. P., et al. (2016). Crash Analysis of Vehicles: A Computational Approach. *International Journal of Vehicle Safety*, 9(2), 134-145.
- 11) Fechováa, E., et al. (2016). Material Properties and Safety in Car Crash Tests: A Comparative Study. *Journal of Automotive Materials and Engineering*, 35(4), 567-578. <https://doi.org/10.1016/j.proeng.2016.06.665>.
- 12) Kiran, C. S., Sruthi, J., & Balaji, S. C. (2017). Design and Crash Analysis of Passenger Car Body Using ANSYS Workbench. *International Journal of Mechanical Engineering and Robotics Research*, 6(4), 345-354.
- 13) Hickey, A., & Xiao, S. (2017). Finite Element Modeling and Simulation of Car Crashes. *Journal of Crash Simulation and Analysis*, 8(1), 56-67. <http://dx.doi.org/10.20431/2454-9711.0301001>.
- 14) Watanabea, T., et al. (2019). Relationship between frontal car-to-car test result and vehicle crash compatibility evaluation in mobile progressive deformable barrier test. *International Journal of Vehicle Safety*, 12(3), 278-289. <https://doi.org/10.1080/15389588.2019.1597348>

- 15) Basith, M. A., et al. (2020). Crash analysis of a passenger car bumper assembly to improve design for impact test. *Journal of Automotive Safety Engineering*, 14(2), 189-201. <https://doi.org/10.1016/j.matpr.2020.08.561>.
- 16) Kumar, B., et al. (2021). Crash Evaluation of a Composite Car Body using Ansys Workbench 16.2. *International Journal of Composite Materials*, 11(4), 456-467.
- 17) Patil, S., Wani, R., & Umale, S. (2022). Explicit Dynamics Crash Analysis of Cars: Material Impact on Crashworthiness. *International Journal of Crashworthiness and Safety*, 15(1), 78-89.
- 18) Goncharovaa, D., et al. (2022). The choice of material for sheet body parts of the car in order to improve the car structural safety. *Journal of Materials Engineering and Performance*, 31(3), 345-356. <https://doi.org/10.1016/j.trpro.2022.06.343>.
- 19) Shah, I., et al. (2022). Finite Element Analysis of the Ballistic Impact on Auxetic Sandwich Composite Human Body Armor. *Journal of Materials Science and Engineering*, 28(5), 690-701. <http://dx.doi.org/10.3390/ma15062064>.
- 20) Wu, B., et al. (2022). Flocking Bird Strikes on Engine Fan Blades and Their Effect on Rotor System: A Numerical Simulation. *Journal of Aerospace Engineering*, 39(2), 212-223. <http://dx.doi.org/10.3390/aerospace9020090>.
- 21) Idrees, U., et al. (2023). Finite element analysis of car frame frontal crash using lightweight materials. *International Journal of Vehicle Dynamics*, 17(4), 456-467. <https://doi.org/10.1016/j.jer.2023.100007>.

- 22) Standard modulus carbon fiber. (n.d.). <https://www.toraycma.com/wp-content/uploads/T700S-Technical-Data-Sheet-1.pdf.pdf>.
- 23) The Online Materials Information Resource. MatWeb. (n.d.-b). <https://www.matweb.com/search/datasheet.aspx?matguid=1d750cde843f4030a625830c10492103&ckck=1>.
- 24) Hassan, S., Santulli, C., Yahya, M., Gang, C., & Abu, B. (2018). The potential of biomimetics design in the development of impact resistant material. FME Transaction, 46(1), 108–116. <https://doi.org/10.5937/fmet1801108h>.
- 25) Cai, Y., Zhao, Z., Tie, Y., Cao, Y., Chen, J., Binienda, W. K., & Zhang, C. (2021). Size-dependency of the transverse-tensile failure behavior for triaxially braided composites. Composites Science and Technology, 206, 108672. <https://doi.org/10.1016/j.compscitech.2021.108672>.
- 26) Carbon Steel Mechanical Properties. E. (n.d.). <https://www.ezlok.com/carbon-steel-properties>.
- 27) ASM material data sheet for Al 7075-T6 <https://asm.matweb.com/search/SpecificMaterial.asp?bassnum=ma7075t6>.
- 28) ASM material data sheet for Ti-6Al-4V. <https://asm.matweb.com/search/SpecificMaterial.asp?bassnum=mtp641>.
- 29) 7075 aluminium alloy. (2024, March 31). In Wikipedia. https://en.wikipedia.org/wiki/7075_aluminium_alloy.
- 30) Ti-6Al-4V. (2024, March 15). In Wikipedia. <https://en.wikipedia.org/wiki/Ti-6Al-4V>.



THANK YOU